SYNTHESIS AND CHARACTERIZATION OF CARBONYL - TUNGSTEN(0) COMPLEXES OF [N,N′-BIS(FERROCENYLMETHYLENE)ETHYLENEDIAMINE]

A THESIS SUBMITTED TO
THE GRADUATE SCHOOL OF NATURAL AND APPLIED SCIENCES
OF
MIDDLE EAST TECHNICAL UNIVERSITY

BY

CÜNEYT KAVAKLI

IN PARTIAL FULFILLMENT OF THE REQUIREMENTS
FOR
THE DEGREE OF MASTER OF SCIENCE
IN
CHEMISTRY

JUNE 2005

Approval of the Graduate School of Natural and Applied Sciences

_____

Prof. Dr. Canan Özgen
Director

I certify that this thesis satisfies all the requirements as a thesis for the degree of Master of Science.

_____

Prof. Dr. Hüseyin İşçi
Head of Department

This is to certify that we have read this thesis and that in our opinion it is fully adequate, in scope and quality, as a thesis for the degree of Master of Science.

_____

Prof. Dr. Saim Özkar
Supervisor

Examining Committee Members

Prof. Dr. Hüseyin İşçi	(METU,CHEM)	_____
Prof. Dr. Saim Özkar	(METU,CHEM)	_____
Prof. Dr. Ahmet Önal	(METU,CHEM)	_____
Prof. Dr. Ceyhan Kayran	(METU,CHEM)	_____
Prof. Dr. Zeynel Kılıç	(Ankara Unv.,CHEM)	_____

I hereby declare that all information in this document has been obtained and presented in accordance with academic rules and ethical conduct. I also declare that, as required by these rules and conduct, I have fully cited and referenced all material and results that are not original to this work.

Name, Last name:

Signature:

ABSTRACT

SYNTHESIS AND CHARACTERIZATION OF
CARBONYL - TUNGSTEN(0) COMPLEXES OF
[N,N′-BIS(FERROCENYLMETHYLENE)ETHYLENEDIAMINE]

Kavaklı, Cüneyt

M.S., Department of Chemistry
Supervisor: Prof. Dr. Saim Özkâr

JUNE 2005, 64 pages

In this study a bidentate ligand containing two ferrocenyl moieties, N,N′-bis(ferrocenylmethylene)ethylenediamine, was prepared by condensation reaction of ferrocenecarboxyaldehyde and ethylenediamine on refluxing in benzene. The molecule was identified by IR, Raman, UV-VIS, ^{1}H-, ^{13}C-NMR spectroscopies. Then, this bidentate ligand was reacted with pentacarbonylbis-(trimethyl)silylethyne)tungsten(0). The ligand substitution reaction in dichloromethane yielded the new complex, tetracarbonyl [N,N´-bis(ferrocenylmethylene)ethylenediamine]tungsten(0) ($W(CO)_4$(BFEDA)). This new complex was isolated from the reaction solution in the form of orange crystals and fully characterized by elemental analysis, IR, UV-VIS, MS, ^{1}H- and ^{13}C-NMR spectroscopies. As a bidentate ligand, N,N´-bis(ferrocenylmethylene)ethylenediamine binds the metal atom in the two cis positions in the pseudooctahedral geometry of the tungsten-complex.

Electrochemistry of the tetracarbonyl [N,N´-bis(ferrocenylmethylene)ethylenediamine]tungsten(0) was studied by cyclic

voltammetry, and controlled potential electrolysis combined with the UV-VIS spectroscopy. One irreversible oxidation and three reversible oxidations were observed in the cyclic voltammogram. One of these reversible and the irreversible oxidations are attributed to tungsten and the other two reversible oxidations to iron centers. It is found that the two ferrocene groups started communication with each other after formation of tungsten-complex.

N,N′-bis(ferrocenylmethylene)ethylenediamine was also reacted with photogenerated pentacarbonyl(tetrahydrofuran)tungsten(0) complex and the pentacarbonyl[N,N'-bis(ferrocenylmethylene)ethylenediamine]tungsten(0) ($W(CO)_5$(BFEDA)) as an intermediate on the route to the tetracarbonyl[N,N'-bis(ferrocenylmethylene)ethylenediamine]tungsten(0) was isolated from the reaction medium in the form of red crystals and fully characterized by, IR, ^{1}H- and ^{13}C-NMR spectroscopies. The conversion of $W(CO)_5$(BFEDA) to the $W(CO)_4$(BFEDA) in dichloromethane by a ring closure mechanism was observed by IR spectroscopy.

Keywords: Ferrocene, Tungsten, Electrochemistry, Ethylenediamine, Diimine.

ÖZ

[N,N´-BİS(FERROSENMETİLEN)
ETİLENDİAMİN] LİGANDININ OLUŞTURDUĞU
KARBONİL-TUNGSTEN(0)
KOMPLEKSLERİNİN SENTEZİ VE KARAKTERİZASYONU

Kavaklı, Cüneyt

Yüksek Lisans, Kimya Bölümü
Tez Yöneticisi: Prof. Dr. Saim Özkâr

Haziran 2005, 64 sayfa

Bu çalışmada, iki ferrosen birimi içeren ve ikidişli bir ligant olan N,N′-bis(ferrosenilmetilen)etilendiamin molekülü benzende geri soğutucu altında ferrosen karboksaldehit ve etilendiaminin kondenzasyon tepkimesiyle hazırlandı. Molekül IR, ^{1}H-, ^{13}C-, UV-VIS, ve Kütle spektroskopi teknikleri yardımıyla tanımlandı. Daha sonra, bu ikidişli ligant pentakarbonil(bistrimetilsililetin)tungsten(0) ile tepkimeye sokuldu. Diklorometanda gerçekleştirilen ligant yerdeğiştirme tepkimesi, tetrakarbonil[N,N′-bis(ferrosenilmetilen)etilendiamin]tungsten(0) kompleksinin oluşumu ile sonuçlandı. Bu yeni kompleks, çözelti ortamından turuncu kristaller şeklinde izole edilebildi ve element analizi, IR, Raman, UV-VIS, MS, ^{1}H- ve ^{13}C-NMR spektroskopileri ile tam olarak tanımlandı. İkidişli N,N′-bis(ferrosenilmetilen)etilendiamin ligandı, metal atomuna iki cis konumundan bağlanarak görünürde oktahedral geometriye sahip olan tungsten kompleksini oluşturdu.

Tetrakarbonil[N,N′-bis(ferrosenilmetilen)etilendiamin]tungsten(0) kompleksinin elektrokimyası dönüşümlü voltametri, UV-VIS spektroskopi ile kombine edilmiş sabit potansiyel elektrolizi ile çalışıldı. Dönüşümlü voltametride bir tersinmez ve üç tersinir yükseltgenme gözlendi. Bunlardan, tersinmez olanı ve tersinir olan yükseltgenmelerden biri tungstene, diğer iki tersinir yükseltgenmenin de merkez demir atomlarına ait olduğu gözlendi. Tungsten kompleksinin oluşmasından sonra, iki ferrosen grubunun birbiri ile elektronik iletişime geçtikleri bulundu.

N,N′-bis(ferrosenilmetilen)etilendiamin ligandı, ayrıca fotokimyasal olarak oluşturulan pentakarbonil(tetrahidrofuran)tungsten(0) ile de reaksiyona sokuldu ve pentakarbonil[N,N′-bis(ferrosenilmetilen)etilendiamin]tungsten(0) kompleksi, tetrakarbonil[N,N′-bis(ferrosenilmetilen)etilendiamin]tungsten(0) kompleksinin oluşumu yolundaki ara kompleks olarak elde edildi. Kırmızı renkteki bu kompleks, IR, ^{1}H- ve ^{13}C-NMR spektroskopileri ile tam olarak tanımlandı. $W(CO)_5$(BFEDA) kompleksinin $W(CO)_4$(BFEDA) kompleksine halka kapanma mekanizmasıyla dönüşümü IR spektroskopisi ile izlendi.

Anahtar Kelimeler: Ferrosen, Tungsten, Elektrokimya, Etilendiamin, Diimin.

To my family

ACKNOWLEDGEMENTS

I would like to express my sincere gratitude to Prof. Dr. Saim Özkâr for his unceasing support, guides, and supervision throughout in this study.

I would like to extend my gratitude to Prof. Dr. M. Ahmet Önal for his close interest and valuable critism especially in the electrochemistry part of this work.

I would also wish to thank to Prof. Dr. Ceyhan Kayran for her precise assistance and valuable critism in the progress of the work.

It is my great pleasure to express my sincere appreciation here to Tülay Aslı Tumay, for her endless moral support, brilliant ideas that helped me so much during this study and the most important one, for her invaluable friendship for over four years.

Last, but not the least, I would like to thank Sanem Koçak, Ceyhun Akyol, Ercan Bayram, Dilek Ayşe Boğa, Ezgi Keçeli, Mehmet Zahmakıran, Önder Metin, Pelin Edinç, Fatma Alper, and Murat Rakap for their caring and encouragement throughout in this work.

TABLE OF CONTENTS

LIST OF TABLES

TABLES

LIST OF FIGURES

FIGURES

CHAPTER 1

INTRODUCTION

Organometallic compounds are usually defined as those that have at least one direct metal-to-carbon interaction. This definition would include metal alkyl compounds such as diethylzinc ($Zn(C_2H_5)_2$) as well as metal carbonyls such as $Ni(CO)_4$ which do not have organic ligands in the usual sense, but which behave much like organic compounds in terms of their volatility, solubility in non-polar organic solvents, and general properties.[1] Organometallic molecules undergo a variety of reactions, such as loss or gain of ligands (or both), molecular rearrangement, formation or breaking of metal-metal bonds or reactions at the ligands themselves.[2]

The first organometallic compound of the transition metals, which has been isolated in 1827 is the Zeise's salt, $K[(C_2H_4)PtCl_3].H_2O$. It is formed when $K_2[PtCl_4]$ in aqueous ethanol is exposed to ethylene; a dimeric $Pt - C_2H_4$ complex with Cl bridges is also formed.[3]

In organometallic compounds, the bond is generally polarized as $M^{\delta+} - C^{\delta-}$. Consequently, the metal atom will be susceptible to nucleophilic attack while the carbon atom will be susceptible to electrophilic attack. In most organometallic compounds, metal-carbon bond has, to a significant degree, covalent character. On the other hand, ionic character of this bond is generally manifested only in compounds of the alkali and alkaline earth metals. The ionic or covalent contribution to the bond depends on ionization potential of the metal, the size of a resulting ion, the ratio of the ionic charge to its radius, and σ-donor, π-donor and π-acceptor properties of ligands and their structure.[4]

Transition-metal carbonyls are among the oldest known classes of organometallic compounds.[5] They are the compounds of various transition metals with carbon monoxide.[6] Since Mond, Langer, and Quincke discovered tetracarbonylnickel in 1890, the field of metal carbonyls has become extremely fertile and a large number of transition metal carbonyls have been prepared.[7]

The metal carbonyl complexes serve as useful starting materials for other organometallic complexes in which a metal-carbonyl system forms an integral part of the structure.[4]Almost all of the transition metals form compounds in which carbon monoxide acts as a ligand. There are three points of interest with respect to these compounds: 1) carbon monoxide is not ordinarily considered a very strong Lewis base and yet it forms strong bonds to the metals in these complexes; 2) the metals are always in a low oxidation state, most often formally in an oxidation state of zero, but sometimes also in a low positive or negative oxidation state; and 3) the 18-electron rule is obeyed by these complexes with remarkable frequency, perhaps 99% of the time.[8] IR spectroscopy is frequently very useful for the characterization of transition-metal carbonyls. Metal complexes containing one or more CO ligands bound to a single metal atom show one or more intense infrared bands between 2200 and 1800 cm^{-1}, which are assigned to the carbon oxygen stretch of the coordinated CO.[9] The intensity is large because $d\mu / dr$, the dipole moment change during vibration is large, thanks to the polarization of the CO on binding to the metal.[10] Quite often, the symmetry of a metal carbonyl complex is determined simply by counting the number of infrared bands. The expected number of IR-active bands can be derived by means of group theory.[11]

Information about the nature of ligand substitution events at low-valent transition-metal centers is useful in systematic organometallic synthesis and in the design of homogeneous catalytic processes. There are many processes that are homogeneously catalyzed by organometallic complexes[12] or transition metal carbonyl complexes. Catalytic hydrogenation, hydroformylation (oxo process) are examples of these metal-carbonyl catalyzed processes. As a result, in addition to having an intrinsic interest for chemists, organometallic reactions are also of great interest industrially, especially in the development of catalysts for reactions of

commercial importance.[2]

It was at least fifty years before when Kealy and Pauson working in Pittsburgh, and Miller, Tebboth, and Tremaine, working in England, announced almost simultaneously that they had prepared a stable crystalline, hydrocarbon soluble compound of iron with two cyclopentadienyl groups, unquestionably $(C_5H_5)_2Fe$.[6] These two independent discoveries were both accidental. One resulted from the observation of a yellow crystalline sublimate formed when a mixture of cyclopentadiene and nitrogen was passed over a reduced iron catalyst (at 300 ^{0}C) of the type used synthetic ammonia process, containing oxides of potassium, aluminium and molybdenum. The other resulted from an attempt to couple cyclopentadienyl radicals by treating cyclopentadienyl-magnesium bromide with ferric chloride.[13]

It can be said that the iron atom of bis(cyclopentadienyl)iron is in the +2 oxidation state, that one pair of electrons is involved in the bond to either ring, and that the bond is not localized between a certain carbon atom and the iron atom but is a delocalized linkage of the iron and the entire ring. This type of bond is now termed the sandwich bond by Wilkinson and the ferrocene bond by others. The name ferrocene itself was suggested by Woodward to emphasize the aromatic nature of bis(cyclopentadienyl)iron.[6]

Ferrocene forms orange needle crystals, m.p. 173-174 ^{0}C, b.p. 249 ^{0}C; it is sufficiently volatile to be steam-distilled. Insoluble in water, it dissolves easily in most organic solvents.[13]

Ferrocene-containing complexes are currently undergoing something of a renaissance due to their increasing role in the rapidly growing area of materials science.[14] It has been used in the synthesis of many new materials having interesting properties.[15] For instance, molecules containing ferrocene moiety have been used as homogeneous catalysts[14], molecular sensors[16], molecular magnets[17], non-linear optic materials[18], and liquid crystals[19]. The presence of ferrocene in a molecule is expected to influence its electron transfer ability.[20] It is highly stable

and has a reversible redox characteristic which means that ferrocenyl derivatives are very important electron-transfer systems for molecular electronics owing to its characteristic redox behaviors[21] and they could also be expected to play a key role of an electron chemical probe of the electron-transfer process in biological molecules.[22] Therefore, it was of general interest to study the electronic influence of ferrocenyl substituents in these ligand systems and metal complexes.[23]

Recently, tetracarbonyl metal-diimine complexes are found to be very important in the synthesis of homogenous catalysts. Photolysis of group 6 metal hexacarbonyls in the presence of potentially bidentate diimine type ligands N-N, ultimately results in the formation of the respective $M(CO)_4$(N-N) chelate complexes.[24,25] It has received attention from several investigators who studied the subsequently occuring chelate ring closure with extrusion of the second CO group from initially formed $M(CO)_5$(N-N). In most of these studies, the $M(CO)_5$(N-N) intermediate has been photogenerated in situ from $M(CO)_6$ in the presence of excess N-N ligand, using either short-time, continuous irradiation, or laser flash excitation.[26]

In the light of these informations about ferrocene containing molecules and their corresponding metal complexes, we thought that Group 6 metal-carbonyl complexes of a ferrocene functionalized imine ligand would be of interest for studying the long-range metal-metal interaction through π-conjugation. For this purpose, a bidentate molecule, N,N'-bis(ferrocenylmethylene)ethylenediamine (BFEDA) was chosen and used as a ligand to form complexes of this kind. (Figure 1.1.). This molecule can bind to the metal center through two potentially nitrogen atoms. One of the most important properties of BFEDA molecule is that it contains two ferrocenyl moieties which are isolated from each other; so the whole molecule can be considered as a two electron reservoir. On the other hand, when it is coordinated to a metal center, an electronic communication exists between two iron centers and the central metal atom. The N,N'-bis(ferrocenylmethylene)ethylenediamine has already been isolated,[27] but its coordination behavior has not been intensively described. To date, only some zinc, copper, iron complexes have been reported.[28] The complexes with the Group

6 metals were not known until the recent studies of its chromium[29] and molybdenum[30] tetracarbonyl complexes.

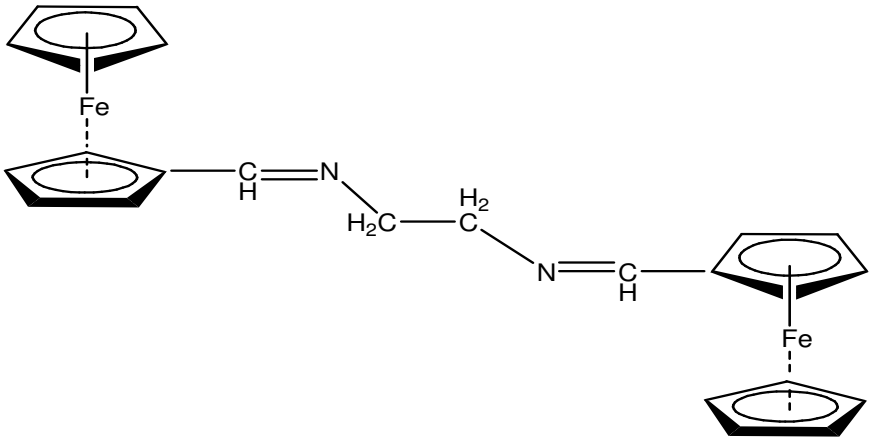

Figure 1.1. The structure of BFEDA

Here, we report the synthesis, characterization and electrochemical study of the tungsten analogue, tetracarbonyl[N,N'-bis(ferrocenylmethylene) ethylenediamine]tungsten(0) ($W(CO)_4$(BFEDA)) complex. $W(CO)_4$(BFEDA) was prepared either by labile-ligand exchange reaction of $W(CO)_5(\eta^2$-btmse) (btmse: bis(trimethyl)silylethyne) complex with BFEDA in CH_2Cl_2 or substitution of thf with BFEDA in the photogenerated $W(CO)_5$(thf). This new complex was isolated from either solution and fully characterized by elemental analysis IR, MS, NMR spectroscopies.

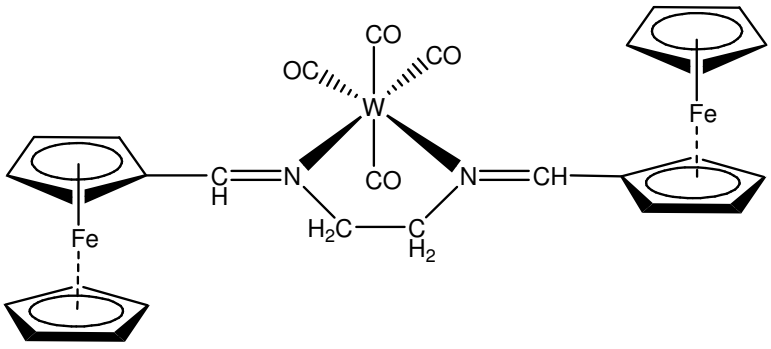

Figure 1.2. The proposed structure of $W(CO)_4$(BFEDA)

We also achieved the isolation of pentacarbonyl[N,N'-bis(ferrocenylmethylene)ethylenediamine]tungsten(0) as intermediate on the route to the tetracarbonyl[N,N'-bis(ferrocenylmethylene)ethylenediamine]tungsten(0).

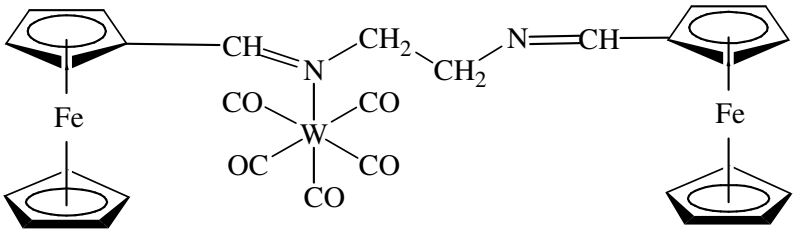

Figure 1.3. The proposed structure of $W(CO)_5$(BFEDA)

The electronic structure of organometallic compounds and their redox behaviours can be examined by electrochemistry. Among the electrochemical methods, perhaps the most suitable technique in determining both the oxidation state and the redox behaviour of the complex in question is cyclic voltammetry, CV. In cyclic voltammetry, the potential is changed as a linear function of time and current that flows in a system is measured.[31]

Combination of spectroscopic and electrochemical studies is a good idea to achieve a full band detailed understanding of the electron transfer properties of organometallic complexes. For example, the combination of UV-VIS electronic absorption spectroscopy and cyclic voltammetry can provide additional useful information about the electronic structure of the organometallic compounds.[32]

The electrochemical behaviour of $W(CO)_4$(BFEDA) was studied by using cyclic voltammetry and differential pulse voltammetry. To find out the number of electrons that were involved in the reduction or oxidation peaks in the cyclic voltammograms, the controlled potential coulometry was used. The changes in solution during the process were followed by UV-VIS spectroscopy. In controlled potential electrolysis, the potential of the working electrode was held at a fixed potential on the plateau of a voltammetric wave, and the electroactive species was oxidized or reduced completely.[33]

CHAPTER 2

BONDING

2.1. Carbonyl Complexes and Metal-Carbonyl Bonding

One of the most commonly encountered ligand in organo-transition metal chemistry is carbon monoxide which forms complexes with these metals known as metal carbonyls. Its primarily mode of attachment to metal atoms is through the carbon atom.[34]

Carbon monoxide is a notoriously poor σ donor. Nonetheless, it will react with transition metals in low oxidation states (usually -1, 0 or +1) to form complexes that are often quite stable with respect to oxidation, dissociation, and substitution. Since the metal is zero-valent, and the CO group is a very poor lone pair donor, it is clear that a simple electrostatic approach can not account for carbonyls.[35] The feature of metal-CO bonding that is presumed to be responsible for this stability is the interaction of filled metal *d* orbitals of π symmetry (t_{2g} in an O_h molecule) with the empty π^* or anti-bonding orbitals of the CO.[36]

The bonding of CO to a metal atom can be explained in MO terms as follows: It is believed to be a σ dative bond as a result of two electron donation of the lone pair on carbon into a vacant metal d-orbital which has σ symmetry. This makes the metal atom electron rich, so in order to compensate this increased electron density, a filled metal d-orbital may interact with empty π^*-orbital on the carbonyl ligand to relieve itself of the added electron density, which is called π - back bonding. As the σ-donation by the carbonyl increases, the strength of the π - back-bonding by the metal increases. This is shown diagramatically as well as through a simple MO picture in Figure 2.1.

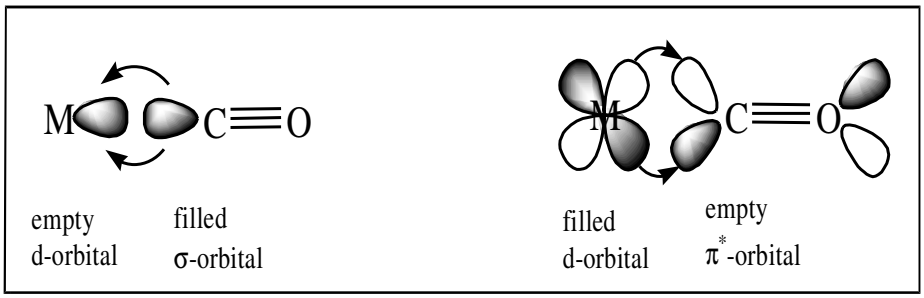

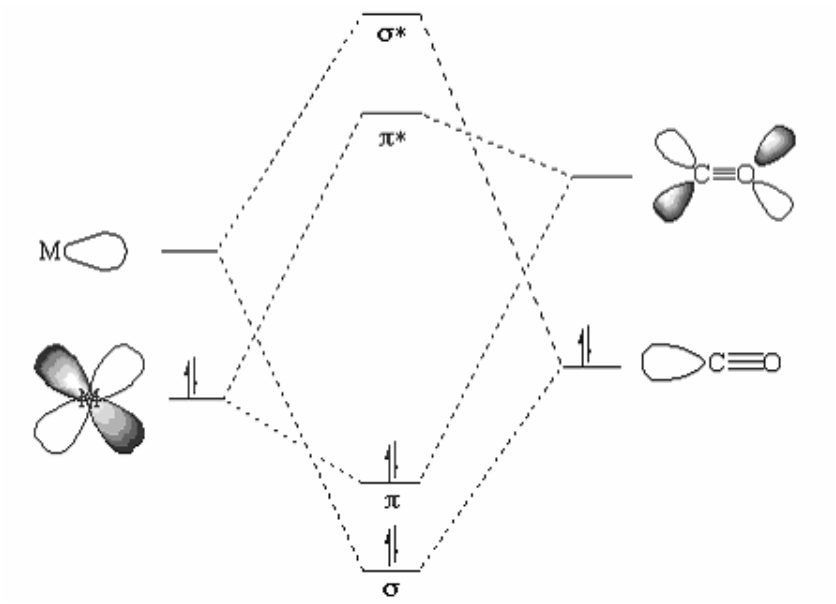

Figure 2.1. Molecular orbital energy level diagram of a L_nM-CO bond. Only frontier orbitals on both fragments are shown.

This mutual reinforcement, which influences the CO bond length, is called synergism.[36]

The strength of the metal carbonyl bonding and the extend of the π bonding depends on the charge on the metal carbonyl or oxidation state of the metal. For instance, the negative charge on the metal atom places a large electron density on the central atom, which means, it will cause a strong metal carbon π-bond due to the extent of electron donation to the carbon atom by the back

donation, by this way metal – carbon bonding will be shorter, while carbon – oxygen bond becomes longer and weaker which directly affects the carbonyl stretching frequency.[37] The stretching frequency of free CO is 2143 cm^{-1}, whereas it is only 2000 cm^{-1} in $Cr(CO)_6$.[36]

Nevertheless, the converse is true if the complex is positively charged. Also other strong σ-donor and π-acceptor ligands attached trans to CO ligand in a mixed metal ligand carbonyl weakens M-CO bond and strengthen C≡O bond simultaneously.[34] This weakening or strengthening is due to the sharing of the same d-orbital by the carbonyl and the L ligand, which is trans to that carbonyl group (π-competition) (Figure 2.2).

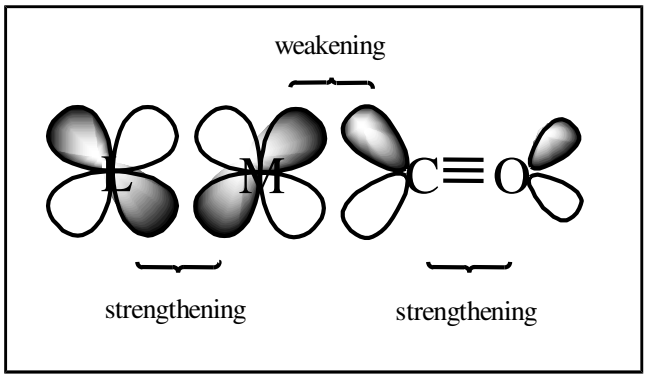

Figure 2.2. Competition for π-bonding in metal carbonyl derivatives.

2.2.Metal-Imine Bonding

Imine compounds, (RCH=NR or R_2C=NR) are formed when aldehydes or ketones react with primary amines. The product can be a mixture of (E) and (Z) isomers. The important issue in this reaction is the formation of water that may cause back-reaction.[38]

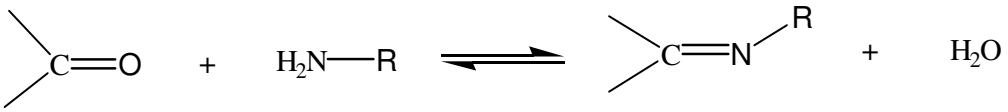

The carbon-nitrogen double bond in an imine molecule is constructed by a σ bond and a π bond. In the MO energy level diagram, (Figure 2.3) there are two σ orbitals (bonding and antibonding) and two π orbitals (bonding and antibonding) for C=N: moiety.

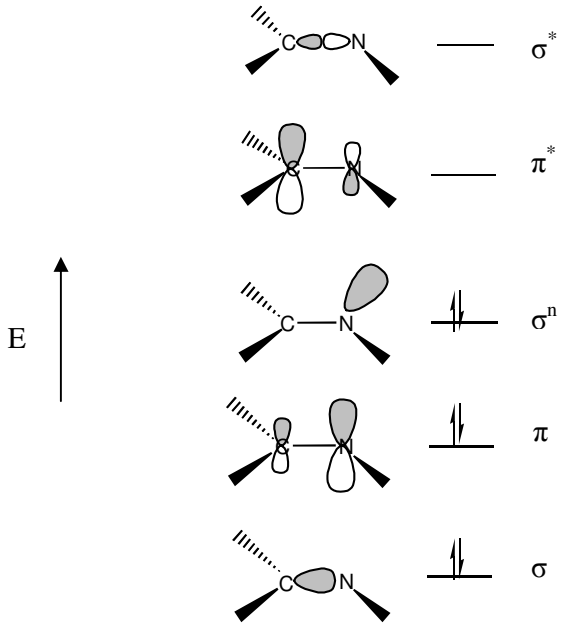

Figure 2.3. The molecular orbital energy level diagram of an imine molecule

Considering the fact that nitrogen is more electronegative than carbon, it can be deduced that the bonding orbitals are mainly localized on the nitrogen atom, while antibonding orbitals belong mainly to the carbon atom. The HOMO of the imine molecule is the nonbonding σ orbital, and the LUMO is the antibonding π^* orbital. A strong σ interaction between metal and the imine ligand should be expected because the HOMO is directed to the dσ orbital of the metal along the bond-axis (Figure 2.4.a). However, the π bonding takes place to the lower extent in comparison with the σ-bonding because the π^* orbital (LUMO) of imine is mainly localized on the carbon atom, that is, the LUMO has its smaller amplitude on the nitrogen (Figure 2.4.b).

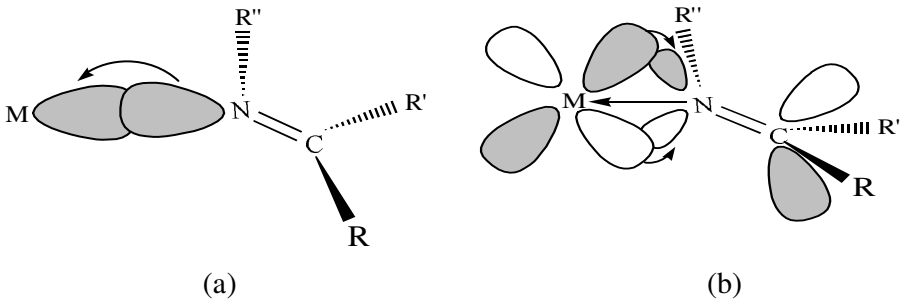

Figure 2.4. Molecular orbital description of the metal-imine bonding;
(a) Metal← imine σ bonding;
(b) Metal → imine π bonding.

These σ and π interactions are synergic. If the π^* orbital of the imine molecule were mainly localized on the nitrogen atom, π bonding would have been much stronger; i.e. imines would have π-accepting ability as strong as the CO ligand. However, the imine ligand is a strong σ-donor and weak π-acceptor, depending on the substituents on the carbon and nitrogen atoms, transition metal and the other ligands coordinated to the metal.

2.3. Metal-Alkyne Bonding

Alkynes (or acetylenes) form complexes with transition metals in a similar way to alkenes and similar bonding schemes can be applied. However, there are some characteristic differences. These can be summarized as follows:[39]

- Alkynes are stronger π-acceptors than alkenes
- C≡C bonds are more reactive than C=C bonds
- Alkynes have 2 orthogonal π^*-systems that can act as 2- as well as 4-electron donor ligands.

According to the MO description of the metal-alkyne bonding which was explained by Dewar[40], Chatt and Duncanson[41] the bonding is assumed to consist of two components as shown in Figure 2.5.

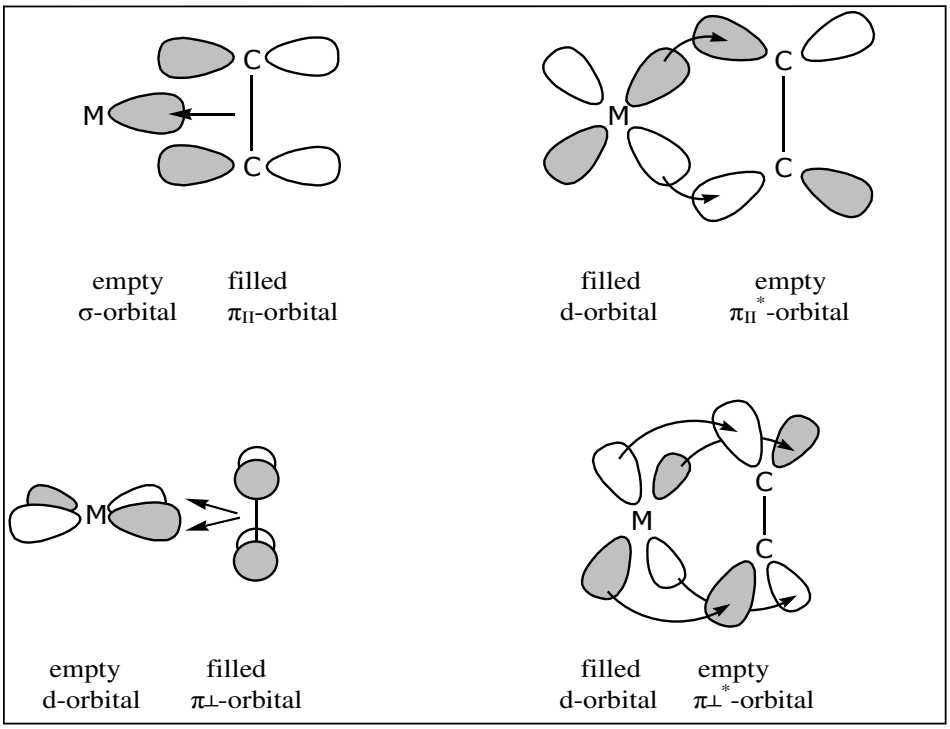

Figure 2.5. Molecular orbital description of the metal-acetylene interaction.

First the formation of σ-bond between the π-orbital of the alkyne and σ-type d-orbital on the metal atom occurs. Here, electron is donated by the alkyne. π back-bonding exists as a result of the overlap of filled π-type d-orbital of the metal and empty π^*-orbital of the acetylene. Same synergic effect is observed between σ- and π-bonds as in the CO case which was mentioned above.

CHAPTER 3

EXPERIMENTAL

3.1. Basic Techniques

Organometallic compounds are very sensitive against the presence of air and moisture. They are somewhat more vulnerable when they are in solutions; the existence of oxygen and water are detrimental for them. For these reasons, synthetic procedures and manipulations should be carried out under dry and deoxygenated atmosphere or under vacuum.

To achieve such a medium during the experiments, an oxygen free dry argon or dinitrogen inert gas line was used. These inert gases are purified before usage (Figure 3.1.). Firstly, the inert gas is allowed to pass through a catalyst (BASF R3.II, Ludwigshafen, Germany) where it is deoxygenated. The temperature of this catalyst is held at 120 ^{0}C by a temperature controller. Then it is passed through molecular sieves to get rid of any moisture and lastly, bubble through glycerine.

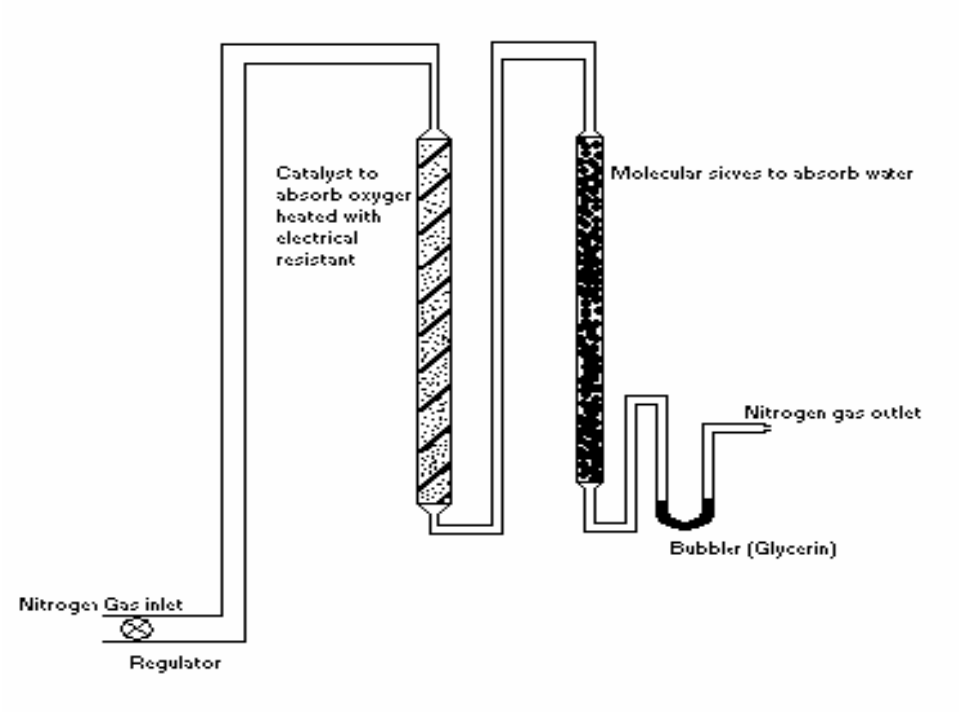

Figure 3.1. Nitrogen gas purification steps

To perform experiments with exclusion of air, vacuum line and schlenk flask, coming from the name of a german chemist William Schlenk who designed it, were used. Schlenk is a glassware equipped with a sidearm for pumping out the air and introducing inert gas in it (Figure 3.2).

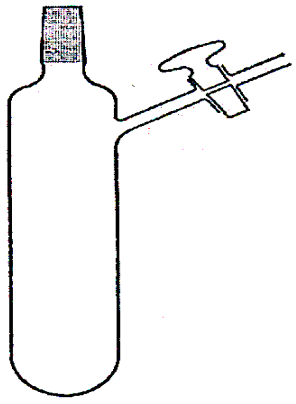

Figure 3.2. Standard schlenk tube

In use, the schlenk ware was first evacuated using a vacuum pump and then filled with inert gas at least three times. All the procedures and handling were applied under argon or nitrogen flow.

All solvents, ferrocene carboxaldehyde, hexacarbonyltungsten and bis(trimethyl)silylethyne (btmse) were purchased from Aldrich. Ethylenediamine was purchased from Merck.

Since solvents are usually in large excess relative to reagents, even minor contaminations with water or oxygen can result in reduced yield or in the worst case, no desired products. For these reason all solvents except CH_2Cl_2 were purified by refluxing over Na before use. During the reflux of thf and toluene, a small amount of benzophenone was used as an indicator. CH_2Cl_2 was refluxed over P_2O_5 for 2 or 3 days before use.

In synthesis of BFEDA, special glassware called Dean-Stark apparatus was used in order to hold the water-benzene mixture away from reaction medium.

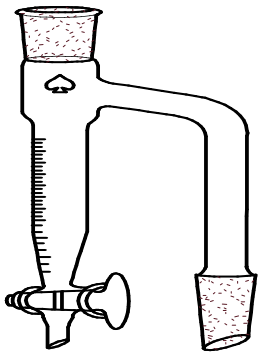

Figure 3.3. Dean Stark apparatus

Photochemical reactions were performed with a special glass apparatus having two parts; an inner part in which a Mercury-Arc Lamp (Hg-Tauchlampe TQ-150) was immersed and an outer part where water was circulated (Figure 3.4).

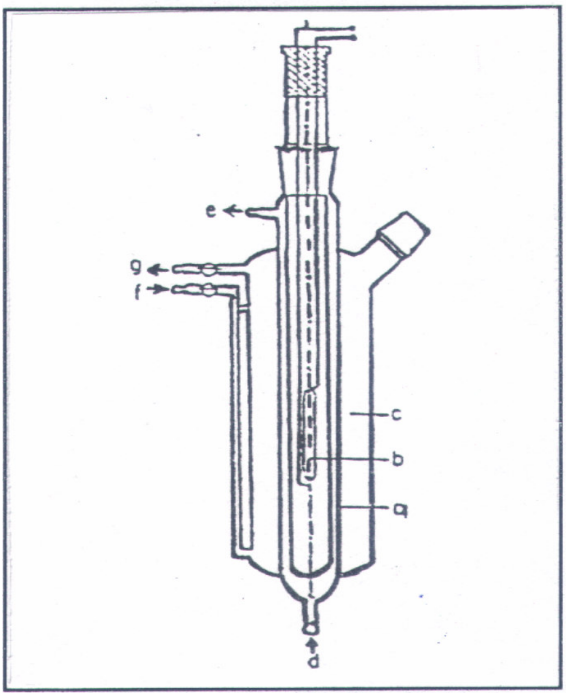

Figure 3.4. The apparatus used for the photochemical reactions

a) inner part
b) Mercury lamp,
c) Outer part
d) Water inlet,
e) Water outlet,
f) Nitrogen gas inlet,
g) Nitrogen gas outlet.

3.2. Physical Measurements

3.2.1 Infrared Spectra

Infrared spectra of the complexes and the BFEDA molecule were recorded from their dichloromethane, toluene, thf or benzene solutions using a Specac IR-Liquid cell with CaF_2 windows on a Nicolet 510 FTIR Spectrometer instrument with Omnic software.

3.2.2 NMR Spectra

The ^{1}H-NMR and ^{13}C-NMR spectra of the BFEDA, $W(CO)_4$(BFEDA) and $W(CO)_5$(BFEDA) were recorded from their d-chloroform, CD_2Cl_2 and d-toluene solutions respectively, on a Bruker-Spectrospin DPX 400 Ultrashield NMR Spectrometer with Avance software. Samples of the complexes were particularly prepared under nitrogen atmosphere. All the chemical shift values were given relative to the signal of TMS used as an internal reference.

3.2.3 Mass spectra

The mass spectrum (MS-FAB) of the $W(CO)_4$(BFEDA) complex was taken on a Fisons VG Autospec instrument at Colorado State University in USA.

3.2.4 Raman Spectra

The Raman spectrum of the BFEDA molecule in solid form was recorded by using a Bruker FRA 106/S Spectrometer with Opus software.

3.2.5 Elemental Analysis

Elemental analysis was performed by using LECO CHNS-932 instrument at Central Laboratory, METU.

3.2.6 UV Spectra

The UV-VIS spectra of the BFEDA molecule and the $W(CO)_4$(BFEDA) complex were measured in CH_2Cl_2 at room temperature on a Hewlett Packard 8452A Model Diode Array Spectrophotometer with UV-Visible ChemStation software.

3.2.7 Cyclic Voltammetry

Cyclic Voltammetry studies of the BFEDA molecule and the $W(CO)_4$(BFEDA) complex were performed in their CH_2Cl_2 solution, in which tetrabutylammonium tetrafluoroborate used as the electrolyte under argon gas atmosphere. SCE (saturated calomel electrode) was used as reference, whereas the platinum bead electrode and platinum wire electrode were used as working and counter electrodes, respectively. HEKA IEEE 488 model potensiostat was used to record voltammetric measurements. Figure 3.5 shows the cell used in the CV studies:

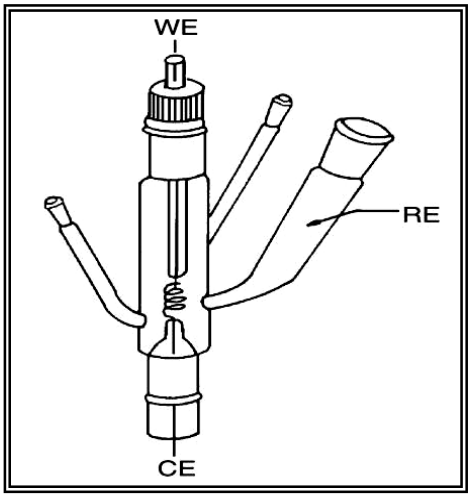

Figure 3.5. Cyclic voltammetry cell

3.2.8 In Situ-Constant Potential Electrolysis

Oxidation and reduction processes of BFEDA and the $W(CO)_4$(BFEDA) complex were carried out at 0°C and at -21°C respectively in their CH_2Cl_2 solutions at the peak potentials observed in cyclic voltammetry with the help of a specific cell shown in Figure 3.6. Changes in the electronic absorption spectra were followed in every 5 mC by using a Hewlett Packard 8452A Model Diode Array Spectrophotometer with UV-Visible ChemStation software.

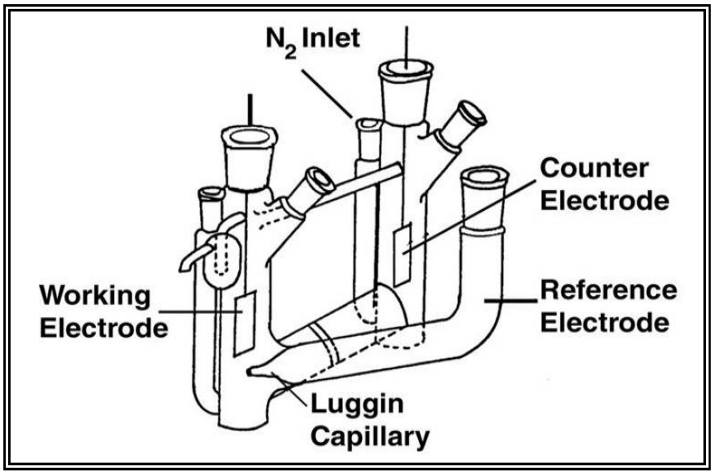

Figure 3.6. Constant potential electrolysis cell; RE: Ag-wire reference electrode; CE: Pt-sieve counter electrode; WE: Pt-wire working electrode.

3.3. Syntheses

3.3.1 Synthesis of N,N'-bis(ferrocenylmethylene)ethylenediamine

N,N'-bis(ferrocenylmethylene)ethylenediamine was prepared by the literature procedure given for the similar ferrocenylimines.[42] Ferrocenecarboxaldehyde (1.01 g, 4.71 mmol) was dissolved completely in 30 mL of benzene at room temperature. Then 0.152 g (2.35 mmol) of ethylenediamine was added to the solution. The flask containing the reaction mixture was connected to a condenser equipped with a Dean-Stark apparatus and refluxed for 4 hours in a glycerine bath. The hot solution was filtered. After cooling down to room temperature, the solution was dried in a rotary evaporator yielding a yellow precipitate. The residue was dissolved in 10 mL of CH_2Cl_2 and left at -35ºC. During this period, yellow crystals formed. After decantation of the mother liquour, the crystals were dried in vacuum. Yield: 0.902 g, 85%. IR (benzene) ν(C=N) = 1644.8 cm^{-1}; UV-VIS (CH_2Cl_2) λ(CT) = 230 nm (ε = 2.965 x 10^4 L/mol.cm) and 274 nm (ε = 1.650 x 10^4 L/mol.cm), λ(d-d) = 330 nm (ε = 0.275 x 10^4 L/mol.cm) and 460 nm (ε= 0.105 x 10^4 L/mol.cm); ^{1}H-NMR ($CDCl_3$) δ = 8.11 (s, 2H, -C**H**=N-), 4.72 (s, 4H, **α**-hydrogens of C_5H_4), 4.33 (s, 4H, **β**-hydrogens of C_5H_4), 4.10 (s, 10H, C_5**H$_5$**), and 3.74 (s, 4H, -C**H$_2$**-C**H$_2$**-) ppm; ^{13}C-NMR ($CDCl_3$): δ = 162.7 (-H**C**=N-), 80.9 (**ipso** carbons of C_5H_4), 70.7 (**α**-carbons of C_5H_4), 69.4(**C$_5$**H$_5$), 68.7 (**β**-carbons of C_5H_4), and 62.7 (-**C**H$_2$-) ppm; CV(CH_2Cl_2) Ox. Pot. = 0.567V, Red. Pot. = 0.462V

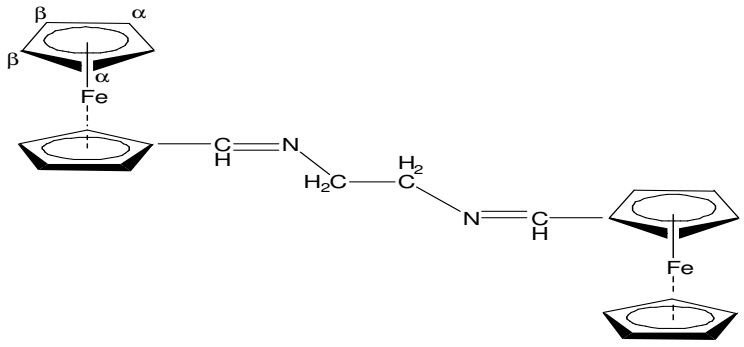

Figure 3.7. The proposed structure of BFEDA.

3.3.2 Synthesis of $W(CO)_5(\eta^2$-btmse)

This complex was prepared photochemically as described in the literature.[45] 1 g hexacarbonyltungsten(0) (2.84 mmol) was dissolved in 200 ml n-hexane and 3.81 ml (17.04 mmol) of btmse (btmse: bis(trimethyl)silylethyne) was added to the solution in photochemical irradiation glassware. The mixture was irradiated for 7 hours at room temperature. The solution was transferred to a schlenk tube and evoporated by help of high vacuum line up to 20 ml. The unreacted $W(CO)_6$ was crystallized out during the volume reduction and filtered off. The rest of the solvent was completely stripped off and the excess of btmse was sublimed over a cold-finger cooled to -30°C by using cryostat under vacuum. The remaining solid dissolved in 15 ml n-hexane and recrystallized at dry ice temperature. Yellow-needle like crystals of $W(CO)_5(\eta^2$-btmse) were obtained. The complex was identified by IR spectroscopy: IR (cyclohexane) ν(CO) = 2080.1, 1988.3, 1960.4, 1953.1, 1938.6 cm^{-1}, $\nu(C\equiv C)$ = 1906.0 cm^{-1}.

3.3.3 Synthesis of Tetracarbonyl[N,N'-bis(ferrocenylmethylene) ethylenediamine]tungsten(0), $W(CO)_4$(BFEDA)

$W(CO)_4$(BFEDA) complex was prepared in two different ways :

0.5 g hexacarbonyltungsten(0) was dissolved in thf and irradiated for 1 hour in photochemical glassware. To the solution containing the photogenerated $W(CO)_5$(thf) complex, 0.64 g BFEDA was added (ligand to metal mol ratio is 1:1) and left for stirring for a day with magnetic stirrer. The replacement of thf with BFEDA was monitored by taking IR spectra from time to time. The mixture was then transferred to a schlenk tube under inert atmosphere and dried in vacuum. The solid residue was dissolved in dichloromethane and the new solution was stirred for a day. The following day, formation of $W(CO)_4L_2$ (L_2: BFEDA) was monitored by IR spectrum. The volume of the solution was reduced by evaporating the solvent in vacuum. The solution was left for recrystallization in deep-freeze at -35 ^{0}C. (0.41 g, 39% yield).

The second way, which gave the best yield is mentioned below:

0.1 g (0.20 mmol) of the $W(CO)_5(\eta^2$-btmse) complex was dissolved in 25 ml dicholoromethane in a schlenk tube. To this solution, 0.09 g (0.20 mmol) of BFEDA was added and stirred for a day with magnetic stirrer. The formation of $W(CO)_4$(BFEDA) with some side products and $W(CO)_6$ was observed from IR spectrum on the following day. The solution was then dried in vacuum and washed with n-hexane for several times to get rid of hexacarbonyltungsten(0) and other complexes. The purification process was continued by recrystallization of the remaining residue in dichloromethane solution at -35 ^{0}C. Yield is 0.097 g, 65%. IR(CH_2Cl_2) ν(CO) = 2005, 1882, 1863, 1819 cm^{-1}; ν(C=N) = 1614 cm^{-1}; UV-VIS (CH_2Cl_2) λ_{max}: 237 (CT) (ε =3.528 x 10^4 L / mol.cm), 250 (CT) (ε =3.372 x 10^4 L / mol.cm), 277 (CT) (ε =1.832 x 10^4 L / mol.cm), 306 (d-d transition of W(0)) (ε =0.964 x 10^4 L / mol.cm), 351 (d-d transition of Fe(II)) (ε =0.110 x 10^4 L / mol.cm), 472 nm (d-d transition of Fe(II)) (ε =0.280 x 10^4 L / mol.cm); CV(CH_2Cl_2) Ox. Pot. = 0.642 V (W/W^+), 0.810 V (Ferrocene/Ferrocenium$^+$), 0.960 V (Ferrocene/Ferrocenium$^+$), 1.07 V (W^+/W^{3+}), Red. Pot. = 0.754 V (Ferrocenium$^+$/Ferrocene), 0.996 V (W^{3+}/W^+); ^{1}H-NMR (CD_2Cl_2) δ = 8.43 (s, 2H, -C**H**=N-), 3.84 (s, 4H, -C**H$_2$**), 4.27 (s, 10H, C_5**H$_5$**), 4.64 (s, 4H, **β**-hydrogens of C_5H_4), 5.16 (s, 4H, **α**-hydrogens of C_5H_4) ppm; ^{13}C-NMR ($CDCl_3$) δ = 214.1 (trans **C**O), 204.9 (cis **C**O), 170.6 (-H**C**=N-), 77.2 (**ipso** carbons of C_5H_4), 72.6 (**α**-carbons of C_5H_4), 72.4 (**β**-carbons of C_5H_4), 69.8 (**C$_5$**H$_5$), 67.5 (**C**H$_2$) ppm.

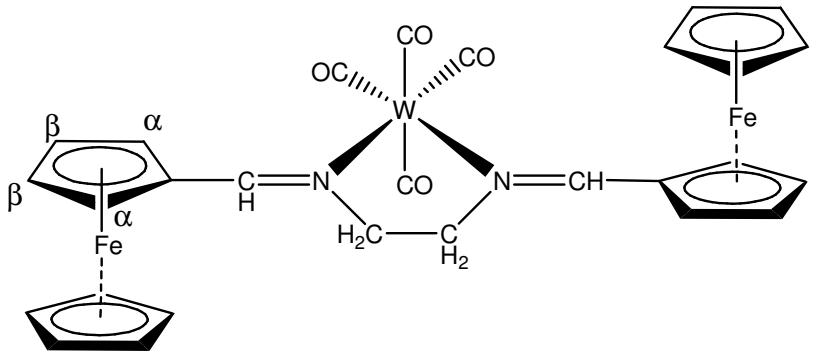

Figure 3.8. The proposed structure of $W(CO)_4$(BFEDA).

3.3.4 Synthesis of Pentacarbonyl[N,N'-bis(ferrocenylmethylene) ethylenediamine]tungsten(0), $W(CO)_5$(BFEDA)

0.1 g (0.20 mmol) $W(CO)_5(\eta^2$-btmse) complex was dissolved in 25 ml toluene in a schlenk tube. To this solution, 0.09 g (0.20 mmol) of BFEDA ligand was added and stirred for 5 hours with magnetic stirrer. During the reaction, it was observed from IR spectrum that both $W(CO)_4$(BFEDA) and $W(CO)_5$(BFEDA) complexes were produced. The solution was dried in vacuum. The solid residue was dissolved in n-hexane to separate $W(CO)_5$(BFEDA) from $W(CO)_4$(BFEDA). The former is soluble while the latter is not soluble. Thus, $W(CO)_5$(BFEDA) complex was taken away from the residue into the solution. The solution was stripped off in vacuum to reduce the volume for crystallization at -35 ^{0}C. Red crystals were obtained (4.6 mg, 3 % yield).

This complex was also isolated from the substitution reaction of thf with BFEDA in $W(CO)_5$(thf). 0.5 g hexacarbonyltungsten(0) was dissolved in thf and irradiated for 1 hour in photochemical glassware. To the solution containing the photogenerated $W(CO)_5$(thf) complex, 0.64 g BFEDA was added (ligand to metal ratio mol is 1:1) and left for stirring for 3 hours with magnetic stirrer. Formation of $W(CO)_5$(BFEDA) in addition to $W(CO)_6$ and $W(CO)_4$(BFEDA) was observed by IR. The solution was transferred into a new schlenk apparatus and dried in vacuum. The soluble $W(CO)_5$(BFEDA) complex was extracted from the solid residue with n-hexane. Purification process was continued by recrystallization in deep-freeze and red crystalline solids (88 mg, 8 % yield) were obtained. IR(n-hexane) ν(CO) = 2067, 1966, 1960, 1922 cm^{-1}; ν(C=N) = 1605, 1652 cm^{-1}; ^{1}H-NMR (d-toluene) δ = 8.51 (s, 1H, hydrogen of -**H**C=N- which is coordinated to the metal center), 8.16 (s, 1H, -**H**C=N-), 4.55 (s, 2H, **α-**hydrogens of C_5H_4), 4.10 (s, 2H, **α'-**hydrogens of C_5H_4), 4.00(s, 5H, hydrogens of C_5**H$_5$** which is closer to the metal-imine bond), 3.91(s, 5H, C_5**H$_5$**), 4.40 (s, 2H, **β-**hydrogens of C_5H_4), 4.08 (s, 2H, **β'-**hydrogens of C_5H_4), 4.02 (s, 2H, closer -C**H$_2$**- hydrogens to the metal-imine interaction) 3.85 (s, 2H, -C**H$_2$**-) ppm; ^{13}C-NMR ($CDCl_3$) δ = 201,6 (trans **C**O), 199.6 (cis **C**O), 175.0 (carbon of H**C**=N which is closer to the metal-imine bond), 162.6 (H**C**=N), 72.7 (**α-**carbons of C_5H_4), 70.3 (**α'-**carbons of C_5H_4), 72.4

(**β-**carbons of C_5H_4), 68.6 (**β'-**carbons of C_5H_4), 69.7 (carbons of $\mathbf{C}_5H_5$ closer to the metal-imine bond), 69.0 ($\mathbf{C}_5H_5$), 80.6 (**ipso** carbon closer to the metal imine bond), 74.1 (**ipso** carbon farther to the metal imine bond), 62.9(closer -$\mathbf{C}H_2$-carbons to the metal-imine bond), 59.9 (-$\mathbf{C}H_2$-).

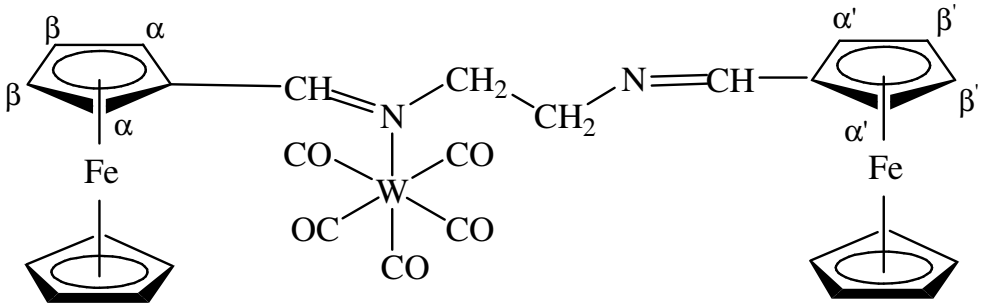

Figure 3.9. The proposed structure of $W(CO)_5$(BFEDA).

CHAPTER 4

RESULTS AND DISCUSSION

4.1. Synthesis and Characterization of BFEDA

BFEDA was synthesized in a similar way that is used for most ferrocenylimines.[27] First, ferrocenecarboxaldehyde was dissolved in benzene and to this solution ethylenediamine was added dropwise. The mixture was refluxed at room temperature for 4 hour with a dean-stark apparatus in a glycerine bath. The reason for using dean-stark is to hold the water-benzene azeotropic mixture away from the reaction medium. The formation of the molecule was observed by IR spectroscopy. From the IR spectrum, it was clearly seen that the peak at 1685 cm^{-1} belonging to the CO stretching of aldehyde group decreased gradually and disappeared ultimately, while a new one at 1644 cm^{-1} due to the stretching of C=N bond grew in. After the reaction was completed, the solution was cooled down and evaporated by rotary-evaporator. The residue was dissolved in dichloromethane and recrystallized at -35 ºC.

The yellow crystals of BFEDA were identified by using IR, Raman, NMR and UV-VIS spectroscopic techniques. In the IR spectrum (Figure 4.1.), the characteristic peak of -C=N- group is seen at 1644 cm^{-1} as it is expected.

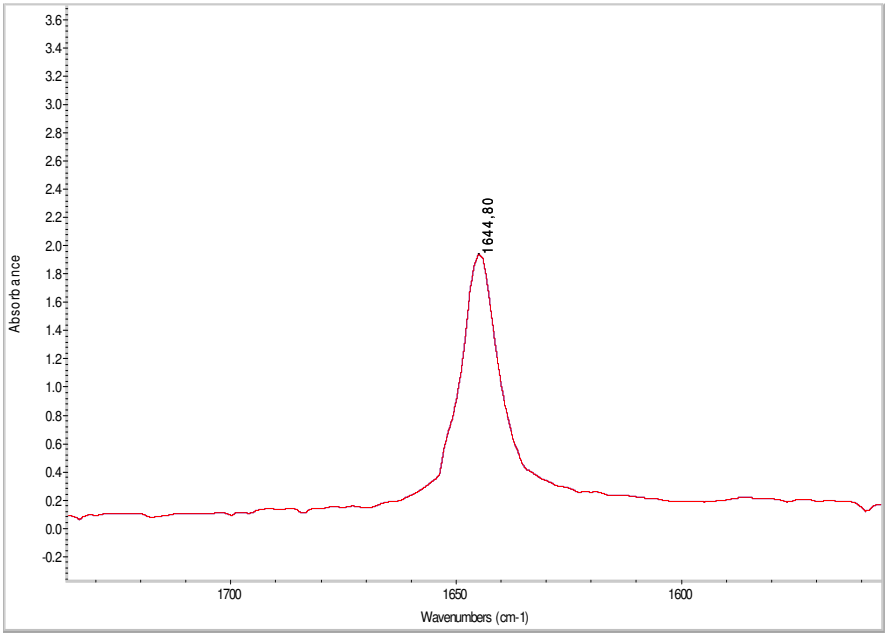

Figure 4.1. Infrared spectrum of N,N'-bis(ferrocenylmethylene)ethylenediamine taken in CH_2Cl_2 at room temperature.

There are two different stretching modes of BFEDA molecule according to the zig-zag shape of the two imine bonds as shown in Figure 4.2. One of them is Raman active, while the other one is IR active. This is because, for a molecule with an inversion center, it is not possible for a vibration to be active in both IR and Raman. This rule was proved for BFEDA molecule; each of IR and Raman spectra taken in solid form of the ligand gives a single absorption band at 1640 and 1644 cm^{-1} for symmetric and antisymmetric C=N stretching modes, respectively (Figures 4.3. and 4.4.).

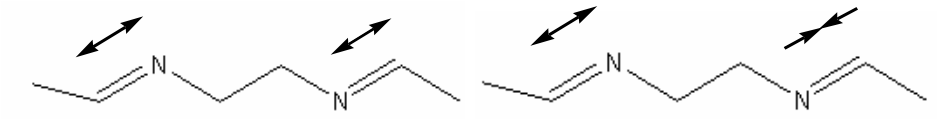

(a) **(b)**

Figure 4.2. Representation of stretching modes in BFEDA
(a) Symmetric stretching, (b) Antisymmetric stretching

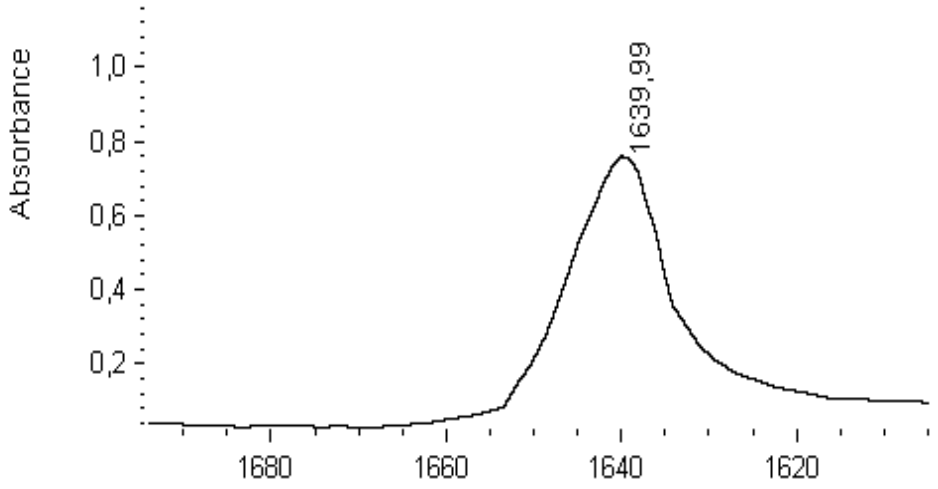

Figure 4.3. Infrared spectrum of BFEDA in KBr pellet.

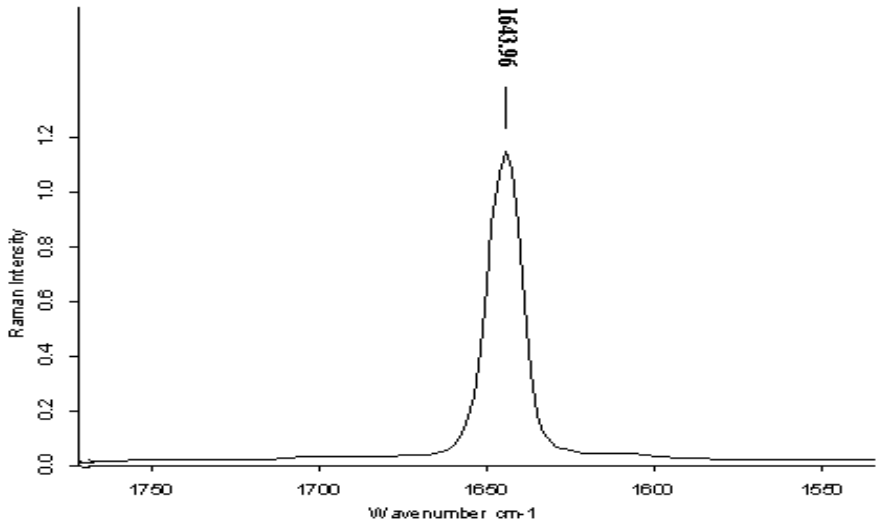

Figure 4.4. Raman spectrum of the BFEDA in solid form.

The ^{1}H-NMR and ^{13}C-NMR spectra also prove the formation of the BFEDA molecule. The hydrogens of both imine groups give a signal at 8.11 ppm. At the ferrocenyl region, three different peaks are observed; at 4.72 and 4.33 ppm

for the monosubstituted and one at 4.10 ppm for the unsubstituted cyclopentadienyl rings with an intensity ratio of 5:2:2, as expected. The protons on the monosubstituted cyclopentadienyl ring resonate at lower field than the five equal protons on the unsubstituted cyclopentadienyl ring, as a result of electron withdrawing effects of the substituents. In addition to this, protons of the monosubstituted ring closer to the electron withdrawing group should be less shielded, so they give a peak at lower region. Lastly, the signal at 3.74 ppm can be assigned to the $–CH_2-$ group.

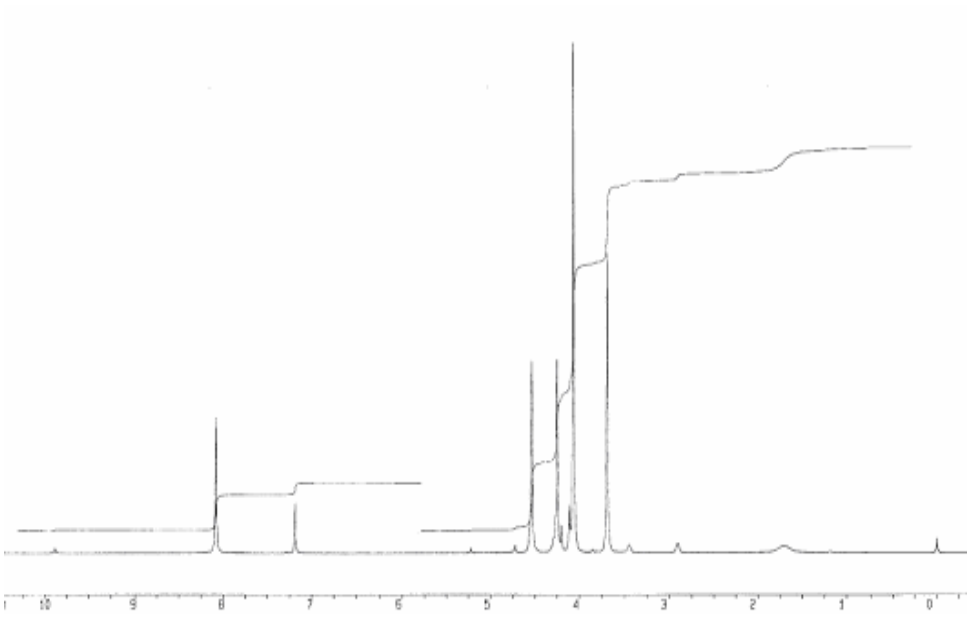

Figure 4.5. ^{1}H-NMR Spectrum of BFEDA in $CDCl_3$

The ^{13}C-{^{1}H}-NMR spectrum of BFEDA shows a peak at 162.7 ppm which can be assigned to the imine carbons. Three signals at 80.9, 70.7 and 68.7 ppm belong to the three different carbons, ipso, α and β of the monosubstituted ring. The ipso carbon is the closest to the electron withdrawing group, so it is the most deshielded carbon, giving a signal at lower magnetic field. A similar comparison can be made for the α and β carbons; α-carbons are closer to the imine groups than β carbons, so they resonate at lower field. The unsubstituted ring carbons resonate at 69.4 ppm. The ratio of the intensities of the peaks is 1:2:2:5, respectively. Lastly, the methylene carbons give a signal at 62.7 ppm.

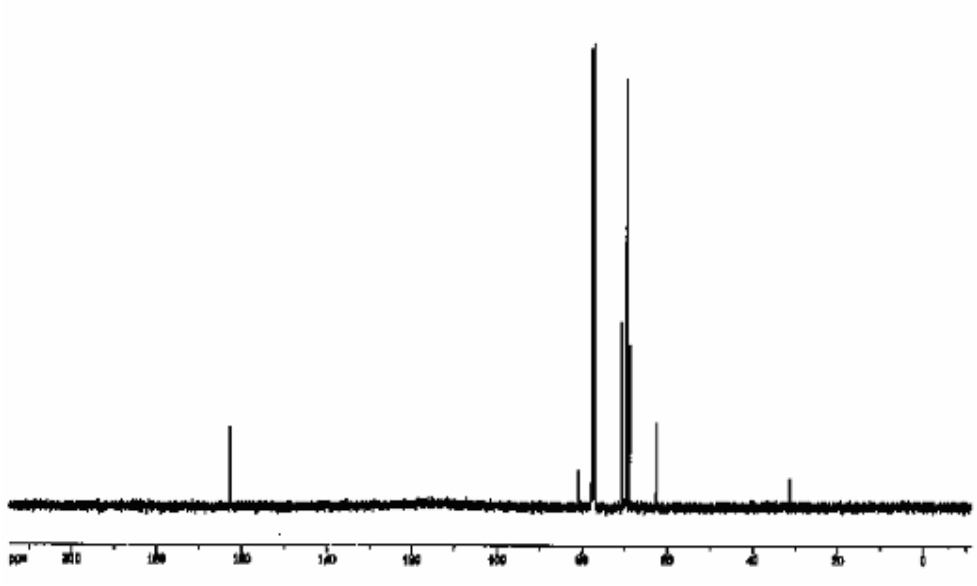

Figure 4.6. ^{13}C-{^{1}H}-NMR Spectrum of BFEDA in $CDCl_3$

Figure 4.7 shows the UV-VIS spectrum of the BFEDA taken at room temperature in CH_2Cl_2. There are four absorption bands at 230, 274, 330 and 460 nm.

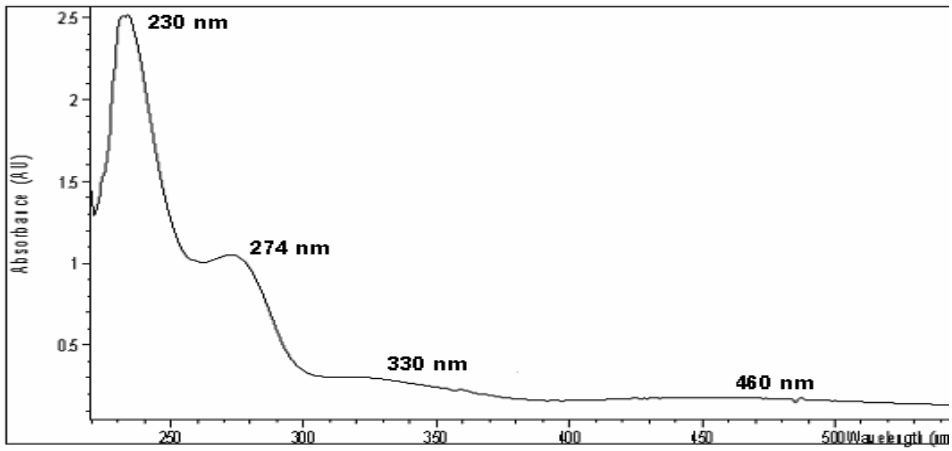

Figure 4.7. UV-VIS spectrum of BFEDA in CH_2Cl_2 taken at room temperature

The bands at 230 and 274 nm can be assigned as charge transfer transitions, when they are compared with the charge transfer bands of free ferrocene (free ferrocene has three charge transfer bands at 265, 239 and 200 nm and two d-d transitions at 458 and 324 nm).[43] The two bands at 330 and 460 nm can be assigned as d-d transition of iron (II) center in the BFEDA molecule.

Cyclic Voltammogram of BFEDA exhibits a reversible oxidation peak at 0.567 V, and a reduction peak at 0.462 V (Figure 4.8). For a single, reversible electron transfer, the half of the difference in cathodic and anodic peak potentials must be around 55-60 mV.[44] Note that this difference is 52 for BFEDA, which indicates that a reversible one-electron transfer reaction occurs during the oxidation process.

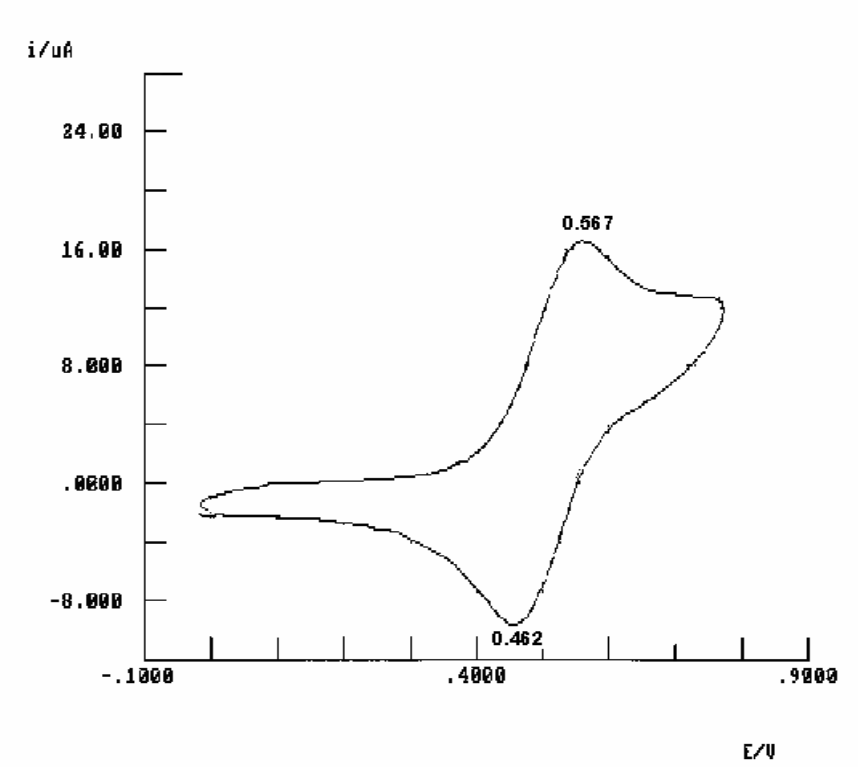

Figure 4.8. CV of BFEDA in CH_2Cl_2 solution at room temperature. Electrolyte: tetrabutylammonium tetrafluoroborate. Reference electrode: Ag wire

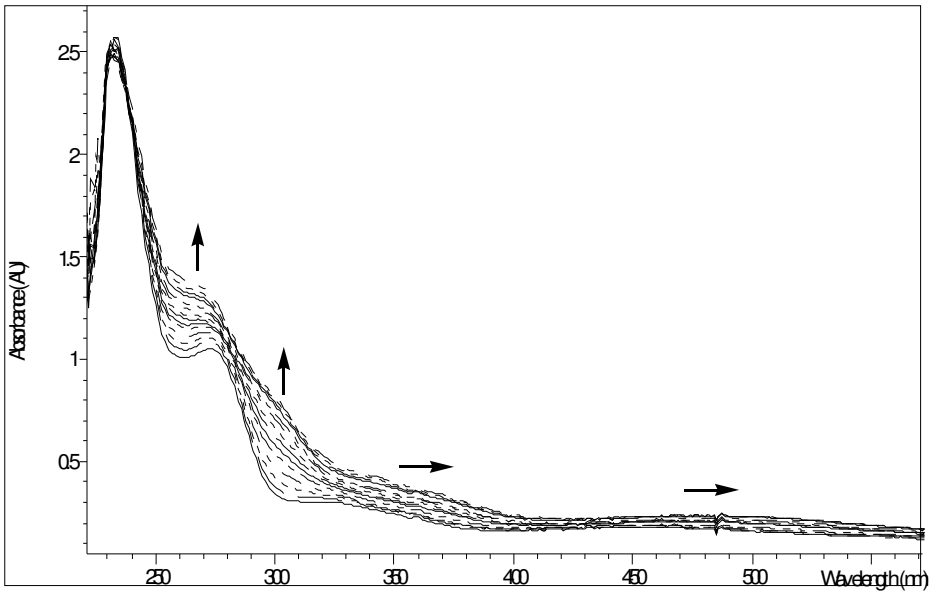

Figure 4.9. The UV-VIS spectra of BFEDA recorded during its electrolytic oxidation in CH_2Cl_2 solution, electrolyte, tetrabutylammonium tetrafluoroborate (TBATFB).

Figure 4.9. shows the UV-VIS spectra recorded during the oxidation of the BFEDA molecule. The oxidation was carried out at the peak potential read from the CV of the molecule. Ag-wire was used as reference electrode during the experiment. While the oxidation continued, the bands at 330 and 460 nm shifted towards lower energies and two new bands, at 268 and 300 nm formed. From the integration of CV and electrolysis, it is concluded that the electron removal happens at the Fe centers; Fe^{2+} to Fe^{3+}. Removal of the electrons from the Fe centers does not differ from each other. Two iron centers are far from each other so; there is no possibility of any electronic communication between them. Thus, we see only one oxidation peak for the two ferrocenyl moieties in the cyclic voltammogram of the BFEDA molecule.

4.2. Synthesis and Characterization of $W(CO)_4$(BFEDA)

Although this complex was synthesized in two different substitution reactions as described in the experimental section, the best yield was obtained by the thermal substitution reaction of bis(trimethylsilyl)ethyne (btmse) in the $W(CO)_5(\eta^2$-btmse) complex with BFEDA in CH_2Cl_2. $W(CO)_5(\eta^2$-btmse) complex is known as a good transfer reagent to prepare variety of $M(CO)_4L_2$ or $M(CO)_5L$ compounds because the metal-alkyne bond is very labile towards substitution in the presence of a potential ligand.[45] In addition, btmse provides stability for $M(CO)_5$-moiety, just enough to be isolated.

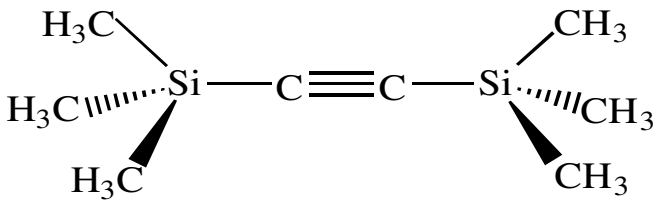

Figure 4.10. Bis(trimethylsilyl)ethyne (btmse)

$W(CO)_5(\eta^2$-btmse) was prepared by irradiating $W(CO)_6$ in the presence of btmse in n-hexane solution for 7 hours.

$$W(CO)_6 + \text{btmse} \xrightarrow[\text{n-hexane, -CO}]{h\nu,\ 7h} W(CO)_5(\eta^2\text{-btmse})$$

Thermal substitution of $W(CO)_5(\eta^2$-btmse) with BFEDA was performed in dichloromethane solution at room temperature by stirring for a day. Following day, the solution was dried in vacuum and washed with n-hexane. The reason of using n-hexane as solvent is that hexacarbonyltungsten(0) and $W(CO)_5$(BFEDA) complexes are soluble in n-hexane, while $W(CO)_4$(BFEDA) complex is not soluble.

$$W(CO)_5(\eta^2\text{-btmse}) + \text{BFEDA} \xrightarrow[CH_2Cl_2]{\text{room T.}} W(CO)_4(\text{BFEDA})$$

Although the ligand exchange of $W(CO)_5$(thf) with BFEDA can also provide the formation of $W(CO)_4$(BFEDA), there were two disadvantages of using substitution reaction of $W(CO)_5$(thf) with BFEDA for the preparation of $W(CO)_4$(BFEDA). First, the solution could not be brought to the dryness even in vacuum, thus, no solid residue could be obtained to purify. Second, many side products including $W(CO)_5$(BFEDA) and $W(CO)_6$ complexes were formed in remarkable amount. These made the isolation of the desired complex difficult and decreased the yield.

IR spectra of the $W(CO)_4$(BFEDA) complex shows four absoption bands in the carbonyl region at 2005, 1882, 1863, 1819 cm^{-1}, which indicates that complex has a local C_{2v} symmetry for $W(CO)_4$ fragment with CO stretching modes of $2A_1 + B_1 + B_2$.[45]

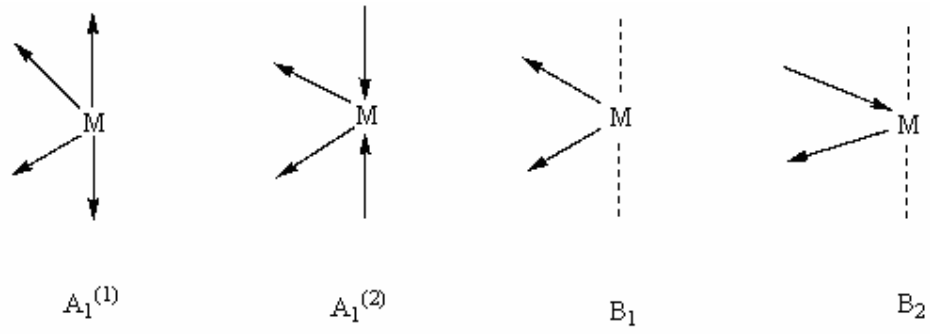

Figure 4.11. The CO stretching vibrational modes in cis-$M(CO)_4$(BFEDA).

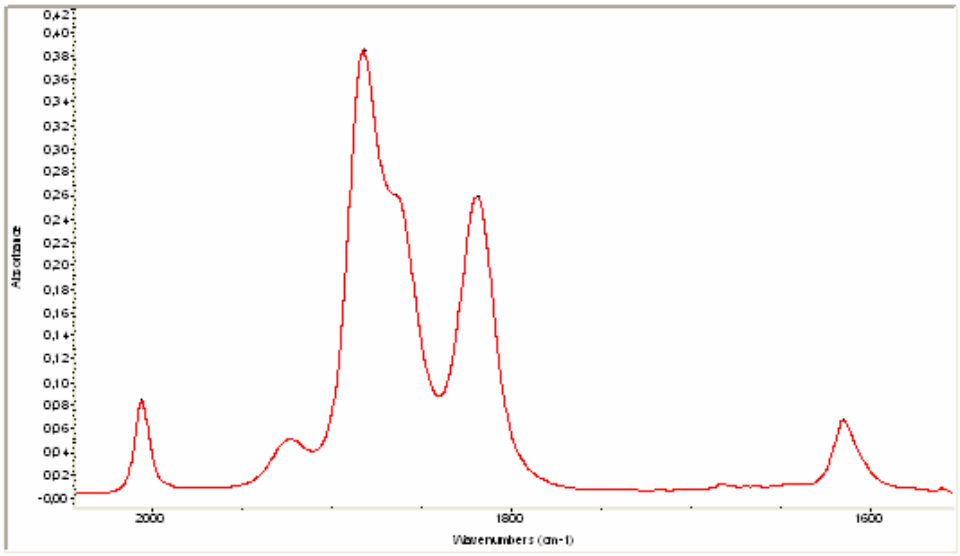

Figure 4.12. The IR Spectrum of $W(CO)_4$(BFEDA) in CH_2Cl_2 measured at room temperature.

The additional absorption band at 1614 cm^{-1} belongs to C=N stretching of the imine group. Remember that the free BFEDA molecule has a value of 1644 cm^{-1} for the same C=N stretching. This decrease of 30 cm^{-1} in wavenumber indicates that C=N bond weakens upon coordination to the metal center.

The ^{1}H-NMR spectrum of the $W(CO)_4$(BFEDA) complex shows a pattern similar to that of the free BFEDA molecule except shifts of all peaks to the lower field as a result of electron-withdrawing effect of $W(CO)_4$ moiety. The imine hydrogen atoms give a peak at 8.43 ppm. When this value is compared with BFEDA molecule (8.11 ppm), imine proton is somewhat more deshielded when it is coordinated to the metal center. The protons of the substituted ring in the coordinated BFEDA resonate at 5.16 ppm (H_α), and 4.64 ppm (H_β). Unsubstituted ring protons give a singlet at 4.27 ppm. The ratio of the protons on the cyclopentadienyl rings is 2:2:5. See that the α protons, which are closer to the imine group than β protons, are more deshielded, thus shift towards lower magnetic field. This is because of the electron withdrawing ability of the imine moiety. Finally, the peak at 3.84 ppm belongs to the methylene protons.

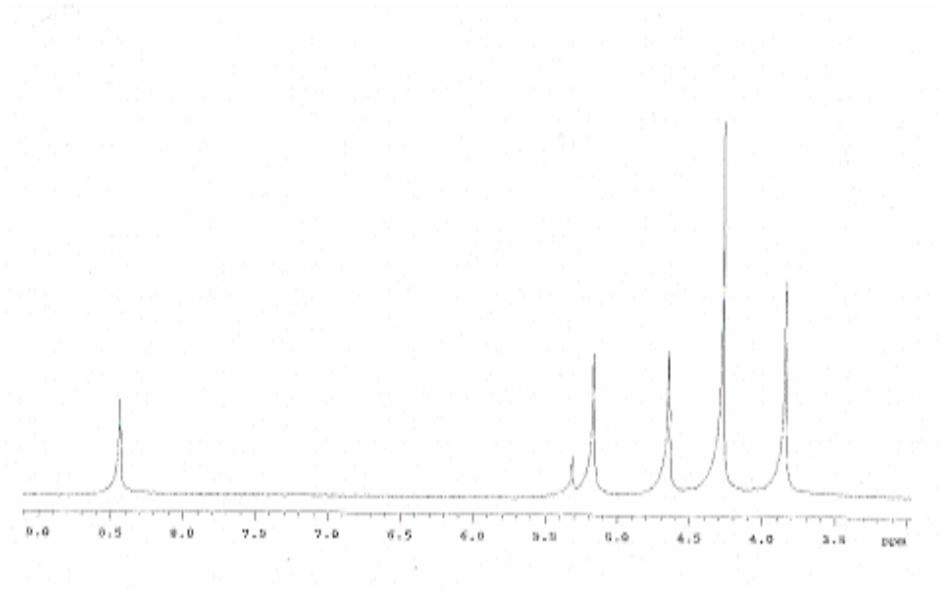

Figure 4.13. The ^{1}H-NMR Spectrum of $W(CO)_4$(BFEDA) in CD_2Cl_2

The ^{13}C-{^{1}H}-NMR spectrum of the $W(CO)_4$(BFEDA) complex shows 3 signals at 77.2, 72.6, 72.4 ppm for the carbon atoms of the substituted ring and one peak at 69.8 ppm for the the carbon atoms of the unsubstituted ring. The imine carbon atoms resonate at 170.6 ppm. Signals at 214.1 and 204.9 ppm belong to the equatorial and axial carbonyl groups to the metal – imine bond, respectively. They are in 1:1 ratio in intensity proving the cis-arrangement of the four carbonyl groups. The carbonyl resonances at lower field (δ = 214.1 ppm) is attributed to the CO groups in the equatorial positions, leaving the one at higher field (δ = 204.9 ppm) for the axial CO groups. This is in accord with the previously reported ordering of signals associated with the axial and equatorial CO groups in $M(CO)_4$(α-diimine) complexes, δ(CO-eq) > δ(CO-ax).[46] Finally, methylene carbons give a signal at 67.5 ppm.

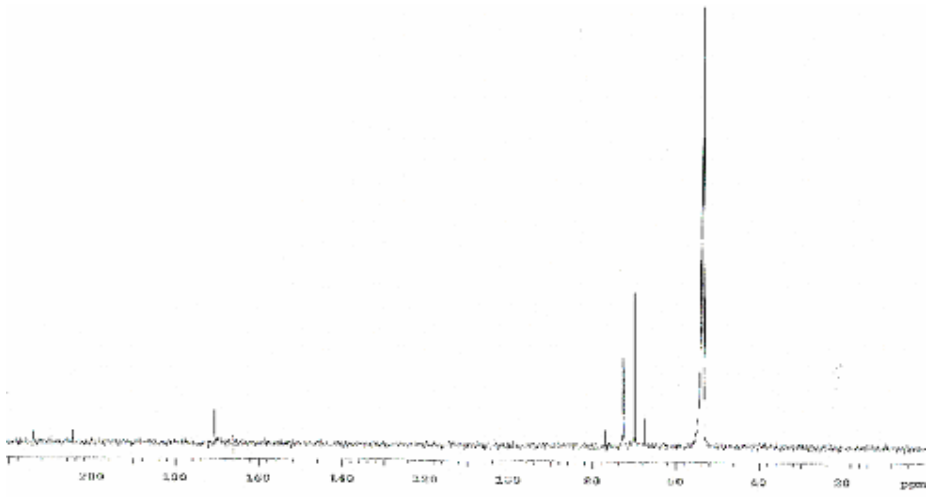

Figure 4.14. ^{13}C-{^{1}H}-NMR Spectrum of of $W(CO)_4$(BFEDA) in CD_2Cl_2

Note that, the ipso carbon of the substituted ring (77.2 ppm) is slightly more shielded than the corresponding carbon of the free BFEDA molecule (80.9 ppm). The reason for this shift may be the π-back bonding between the tungsten metal center and the imine group. When BFEDA is coordinated to the metal center, electrons start to flow toward the metal. Consequently, electron rich metal center starts to donate its electrons back to the imine moiety through π interaction. Since π^* orbital of the imine is mainly localized on the carbon atom, the more populated, imine π^* orbital is attainable for the π interaction with the cyclopentadienyl ring. Thus, the electron density around the ipso carbon increases and its signal shifts to higher magnetic field.

The rest of the carbon atoms are slightly more deshielded than free BFEDA. The coordination shift values of the α and β carbons on the substituted ring are greater than that of carbons of the unsubstituted ring. This can be attributed to the strong interaction of the carbon atoms with the W metal through conjugation. Also, when coordinated, α and β carbons have very similar chemical shifts. This is a result of the delocalization of the electrons on the substituted cyclopentadienyl ring as the electron density decreases. The shifts of the cyclopentadienyl carbon signals toward lower magnetic field are indicative of a σ-donor rather than π-acceptor ability of the BFEDA. As expected from the

closeness of the carbon atoms to the coordination site, the highest coordination shift value belongs to the carbon atom of the imine.

For comparison, the ^{13}C-NMR chemical shifts for the free BFEDA, $W(CO)_4$(BFEDA) and $W(CO)_5$(BFEDA) complexes are listed in Table 4.1.

Table 4.1. ^{13}C-NMR chemical shifts (δ, ppm) of BFEDA, $W(CO)_4$(BFEDA), and $W(CO)_5$(BFEDA). Coordination shift values are shown in parentheses (Δδ, ppm).

	δ(**C**$_{ipso}$)	δ(**C**$_{unsubs}$)	δ(**C**$_{\alpha}$,**C**$_{\alpha'}$)	δ(**C**$_{\beta}$,**C**$_{\beta'}$)	δ(H**C**=N)	δ(**C**H$_2$)
BFEDA	80.9	69.4	70.7	68.7	162.7	62.7
$W(CO)_4$(BFEDA)	77.2 (-3.7)	69.8 (0.4)	72.6 (1.9)	72.4 (3.7)	170.6 (7.9)	67.5 (4.8)
$W(CO)_5$(BFEDA)	80.6 (-0.3) 74.1 (-6.8)	69.7 (0.3) 69.0 (0.4)	72.7 (2.0) 70.3 (-0.4)	72.4 (3.7) 68.6 (-0.1)	175.0 (12.3) 162.6 (-0.1)	62.9 (0.2) 59.9 (-2.8)

Elemental analysis results for the nitrogen, hydrogen and carbon atoms are given in Table 4.2. Experimental results are very close to the theoretically calculated for $C_{28}H_{24}Fe_2WN_2O_4$.

Table 4.2. Elemental analysis values and theoretical mass percentages of the carbon, hydrogen and nitrogen atoms in the $W(CO)_4$(BFEDA).

ATOM	**EXPERIMENTAL %**	**THEORETICAL %**
CARBON	45.11	44.50
HYDROGEN	3.24	3.20
NITROGEN	3.78	3.74

Mass spectroscopy was used for further characterization of the complex. The spectrum (Figure 4.15.) shows the molecular peak of the complex with unique isotope distribution (m/z = 748). This result is exactly in accord with the theoretical molecular weight, calculated for $C_{28}H_{24}Fe_2WN_2O_4$.

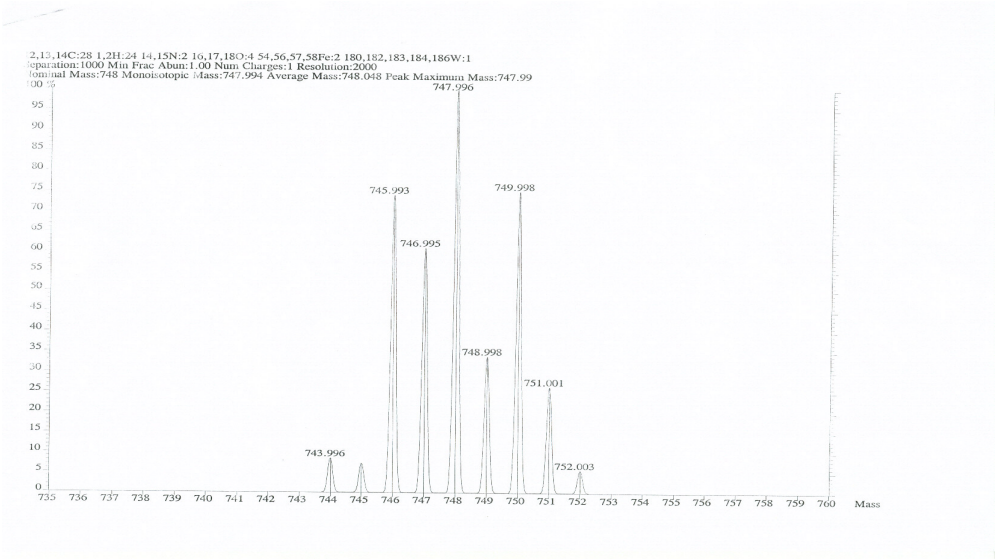

Figure 4.15. Mass spectrum of $W(CO)_4$(BFEDA)

The UV-VIS spectrum (Figure 4.16.) of the $W(CO)_4$(BFEDA) complex shows six absorption peaks. Bands at 237, 250 and 277 nm are assigned to the charge transfer transitions of the ferrocenyl moiety. There exists a d-d transition band of W(0) at 306 nm, whereas the bands at 351 nm and 472 nm belong to the d-d transition of the Fe(II) metal. Note that, although free BFEDA molecule shows only two charge transfer bands, the $W(CO)_4$(BFEDA) complex shows a third one at 250 nm. This band may be assigned to a charge transfer transition from the imine moiety to the tungsten metal.

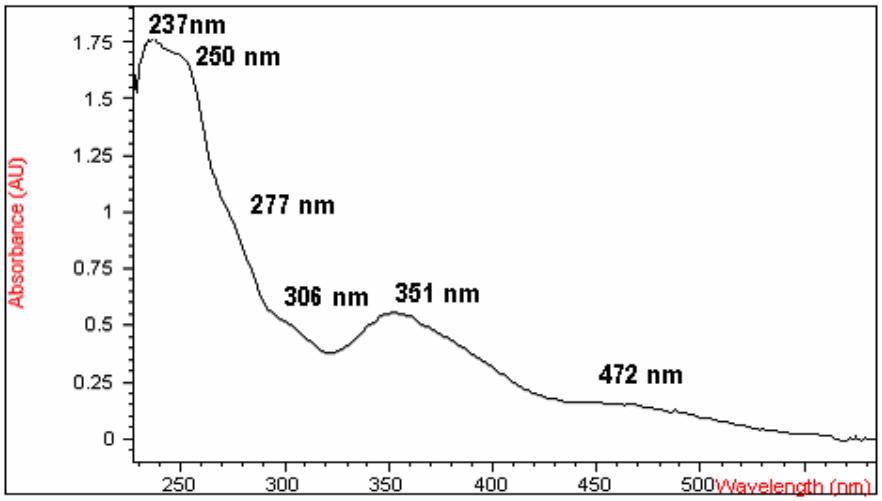

Figure 4.16. UV-VIS spectrum of $W(CO)_4$(BFEDA) in CH_2Cl_2

The electrochemical properties of the $W(CO)_4$(BFEDA) complex was investigated by cyclic voltammetry and differential pulse methods. Four oxidation peaks were observed at 0.642, 0.810, 0.960 and 1.070 V during the anodic scan. The first oxidation peak may be assigned to the oxidation of the tungsten metal center from W(0) to W^{1+} and this oxidation is irreversible. This type of irreversible oxidation for W(0) to W^{1+} have been reported in literature.[47] The reason for this irreversibility may be the poor stability of the complex in the oxidized form at room temperature.

Second and the third peaks show the oxidation of the two Fe centers from Fe^{2+} to Fe^{3+}. Note that two ferrocene moieties are seperated from each other now, unlike the case in free BFEDA molecule. This shows the existence of an electronically communication between them via connection to the tungsten metal center. The weak feature at 1.070 V can be attributed to the oxidation of the tungsten metal center from W^{1+} to W^{3+}, similar to the analogous $Mo(CO)_4$(BFEDA) complex.[30]

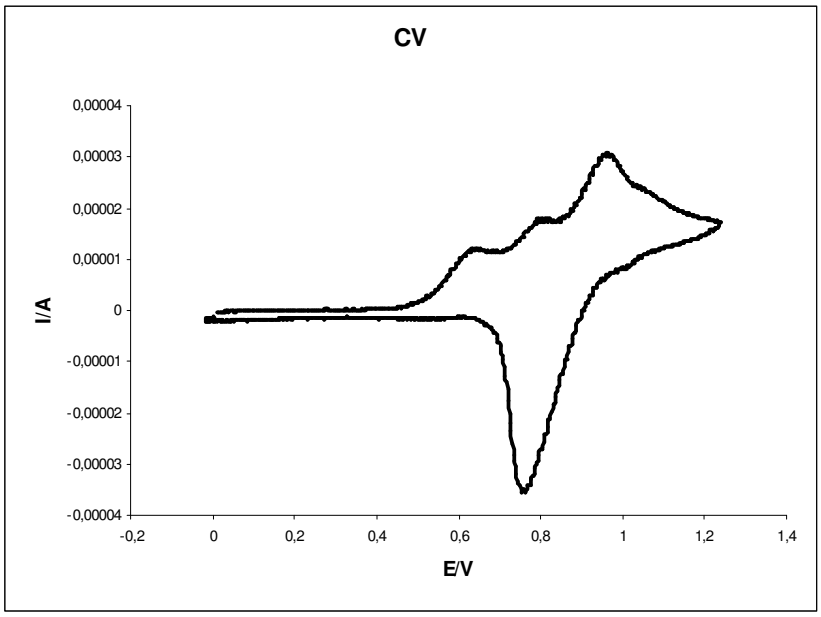

Figure 4.17. CV of $W(CO)_4$(BFEDA) in CH_2Cl_2 solution with saturated calomel reference electrode and the electrolyte, tetrabutylammonium tetrafluoroborate. Scan rate is 100 mV / s.

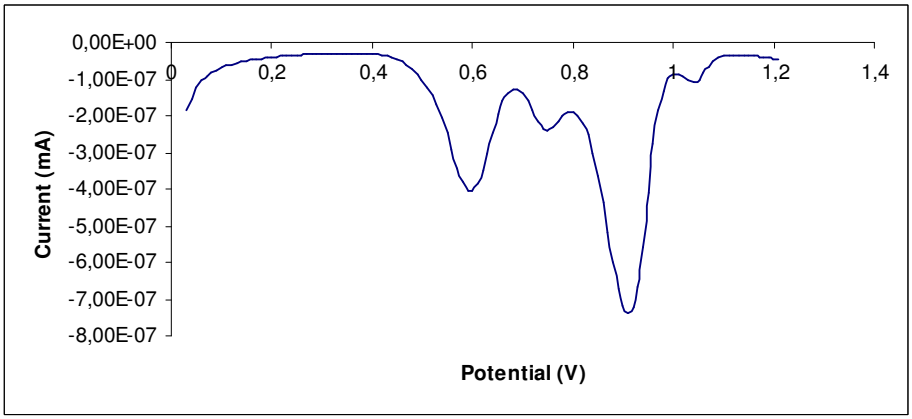

Figure 4.18. Differential pulse voltammogram of $W(CO)_4$(BFEDA) in CH_2Cl_2 solution with SCE reference electrode and the electrolyte, tetrabutylammonium tetrafluoroborate. Scan rate is 50 mV / s.

The reverse scan shows two reduction peaks. The reduction at 0.996 may be related to the reduction of tungsten. The intense reduction peak at 0.754

attributed to the reduction processes of two iron centers.

The electrochemical constant potential oxidation of the $W(CO)_4$(BFEDA) complex was performed in its CH_2Cl_2 solution. In order to minimize the volatalization of the solution and decomposition of the complex, the experiment was carried out at -21 ^{0}C. The spectral changes were followed by in-situ UV-VIS spectrophotometer. The changes in absorption bands are given in Table 4.3.

Table 4.3. Spectral changes in UV-VIS of $W(CO)_4$(BFEDA) during control potential electrolysis in CH_2Cl_2 and TBATFB solution

COMPLEX	C.T.	C.T.	C.T.	d-d transition (W)	d-d transition (Fe)	d-d transition (Fe)
$W(CO)_4$(BFEDA)	237	250	277	306	351	472
$W(CO)_4(BFEDA^+)$	245	------	269	298	367	496
$W(CO)_4(BFEDA^{+2})$	245	------	269	298	373	512
$W^+(CO)_4(BFEDA^{+2})$	250	------	266	299	373	512
$W^{+2}(CO)_4(BFEDA^{+2})$	246	------	267	299	372	521

As it is mentioned before, the oxidation of W(0) to W^{1+} is irreversible. This first step oxidation is thought as a short-lived intermediate, since no change in UV-VIS spectra was observed other than ligand-based oxidation during the oxidation process until the end of first two electron passage. It is believed that W^{1+} undergoes an intramolecular electron transfer and reduced back to W(0), while one Fe metal center is oxidized to ferrocenium cation simultaneously. The spectral changes during two electrons oxidation were similar, so we can deduce that secondly, the other ferrocene moiety was oxidized.

In first two-electron oxidation part, the peaks at 237 and 277 decreased in intensity and shifted to 245 and 269 nm, respectively, while the band at 250 nm disappeared and was not observed throughout the electrolysis again. The d-d transition band of tungsten center at 306 nm also decreased in intensity and shifted to 298 nm. Two bands of Fe centers at 351 and 472 nm shifted to 367 and 496, and then to 373 and 512 nm, respectively. Three isosbestic points can be seen clearly through out this part, which means a straightforward conversion to the products without any side products.

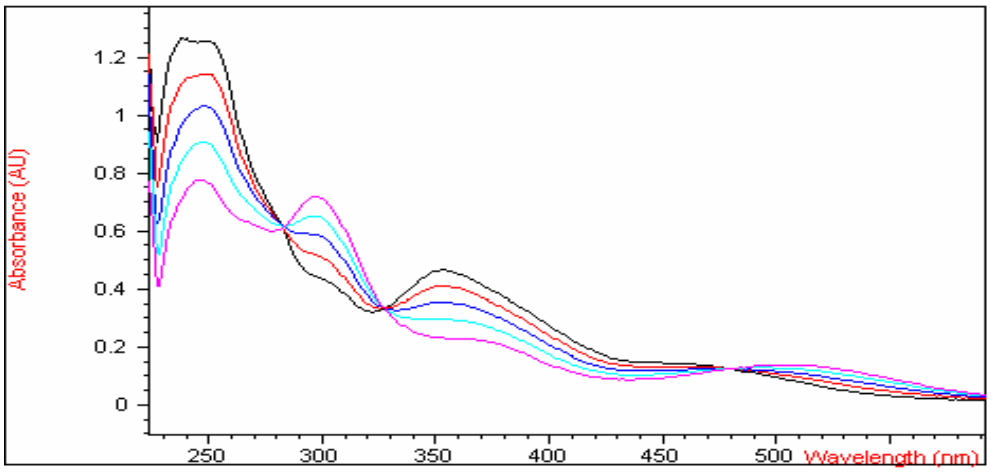

Figure 4.19. UV-VIS spectra of controlled potential oxidation of $W(CO)_4$(BFEDA) at -21 ^{0}C in CH_2Cl_2 and TBATFB solution until two electron oxidations were completed.

After two electron oxidation of the ferrocenyl moiety, the oxidation of tungsten metal center first from W(0) to W^{1+} and then from W^{1+} to W^{3+} was expected. Unfortunately, the experiment was carried on until four electron passage completed as the complex started to decompose. Thus, the fifth electron oxidation could not be accomplished.

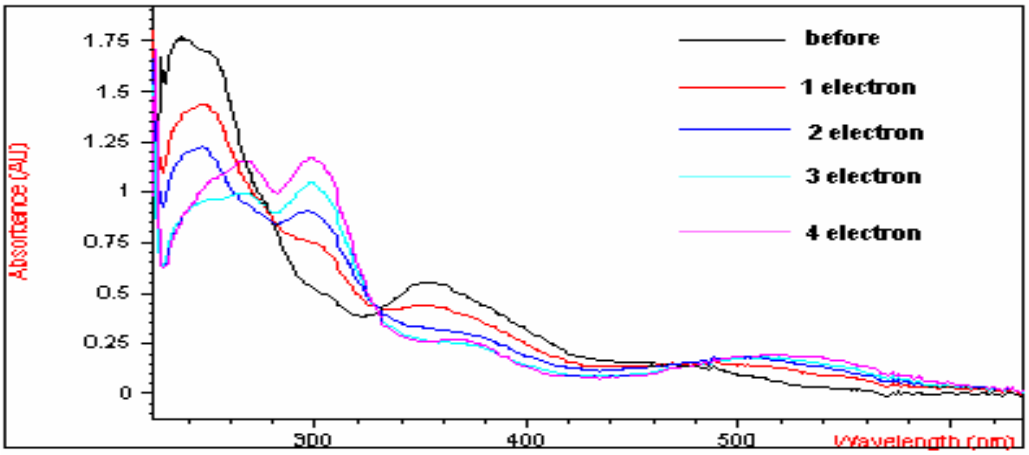

Figure 4.20. UV-VIS spectra of controlled potential oxidation of $W(CO)_4$(BFEDA) at -21 °C in CH_2Cl_2 solution containing the electrolyte, tetrabutylammonium tetrafluoroborate.

The events observed during the electrolysis can be summarized as follows:

1. Oxidation of the tungsten metal from (0) to (+1) and then its immediate reduction back to zero via an intramolecular electron transfer from one of the Fe^{2+} center which becomes Fe^{3+}:

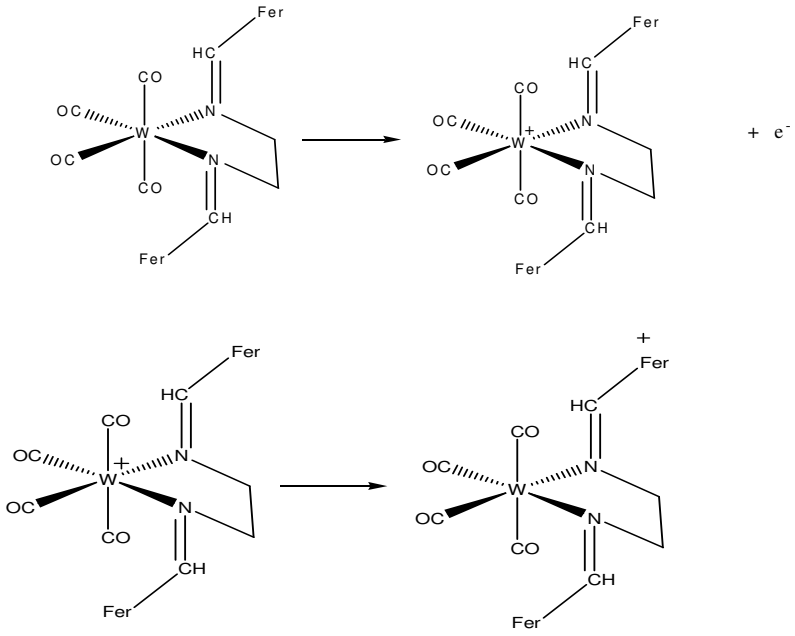

Oxidation of the second iron center from (+2) to (+3):

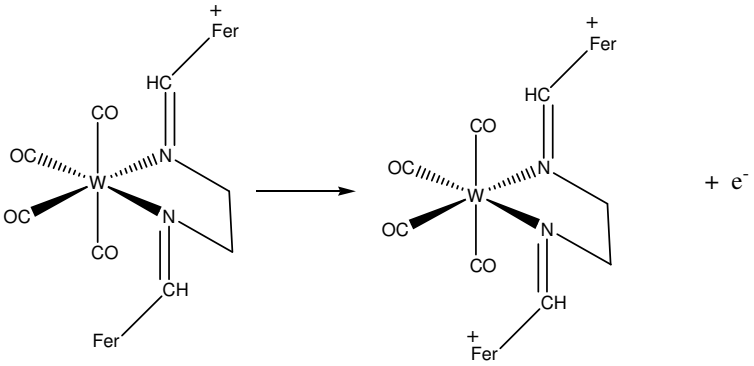

2. Oxidation of the tungsten metal from zero to +1:

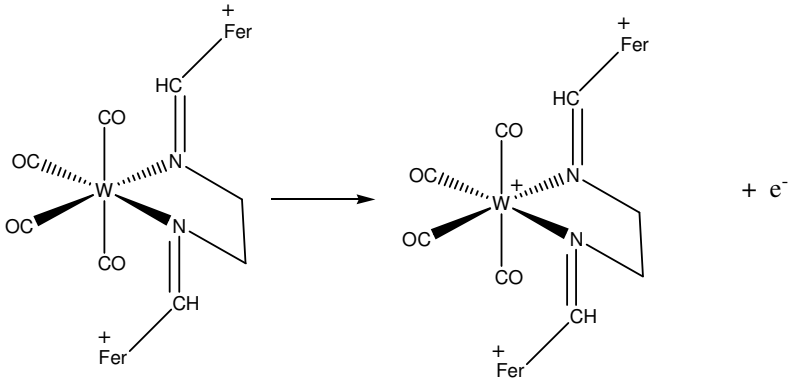

3. Oxidation of tungsten metal from (+1) to (+2):

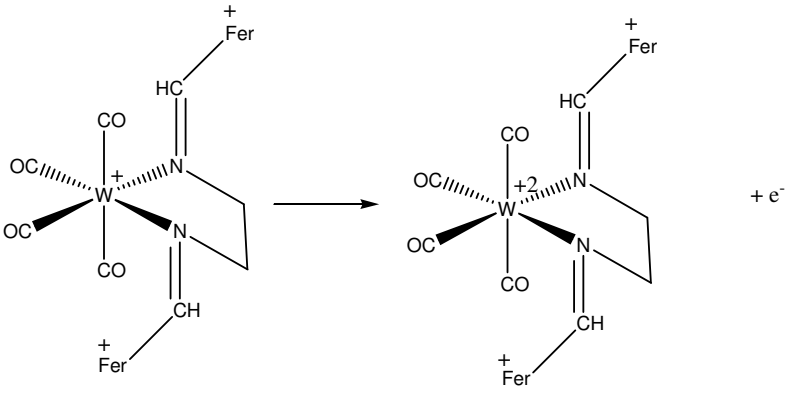

4.3. Synthesis and Characterization of $W(CO)_5$(BFEDA)

$W(CO)_5$(BFEDA) was synthesized by two different substitution reactions as discussed in the experimental section. However, the best yield with the highest purity was obtained after recrystallization of the product from the thermal substitution reaction of thf in the photogenerated $W(CO)_5$(thf) with BFEDA.

$W(CO)_5$(thf) was prepared by direct irradiation of $W(CO)_6$ in thf for one hour. Thf is an easily coordinating ligand, so if it is irradiated longer than one hour, further substitution yields $W(CO)_4(thf)_2$. After one hour irradiation, BFEDA was added into the solution in 1:1 mole ratio with $W(CO)_6$. The substitution reaction was followed by IR spectra. After five hours of stirring, the solution was poured into another schlenk and dried up. The solid residue was dissolved in n-hexane and by this way, $W(CO)_5$(BFEDA) was crystalized from this solution at -35 ^{0}C in deep-freeze.

$$W(CO)_6 \xrightarrow{h\nu,\ 1h} W(CO)_5(THF)$$

$$W(CO)_5(THF) \xrightarrow{BFEDA,\ 5\ h} W(CO)_5(BFEDA) + W(CO)_4(BFEDA)$$

Infrared spectrum of the $W(CO)_5$(BFEDA) complex shows five peaks in the CO stretching region. Thus, the $W(CO)_5$ moiety is assigned to have a local C_{2v} point group with the stretching modes of $3A_1 + B_1 + B_2$.[45]

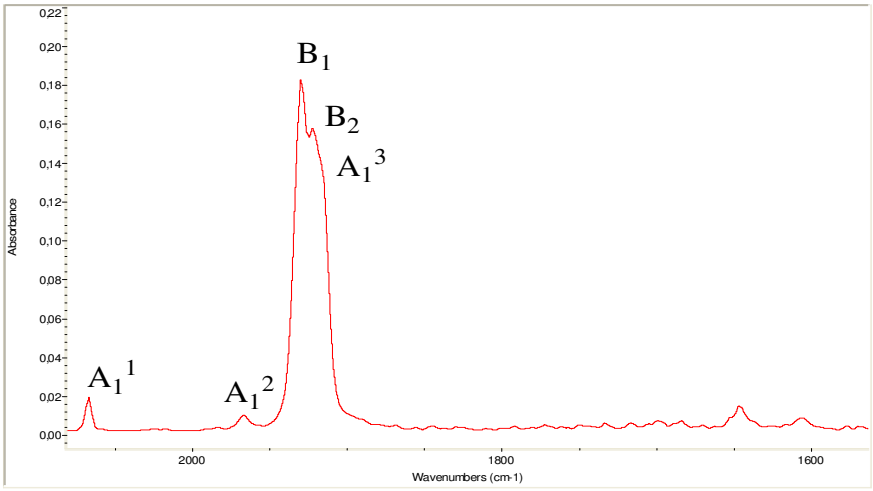

Figure 4.21. IR spectrum of $W(C0)_5$(BFEDA) in n-hexane

Table 4.4. CO stretching modes of $W(CO)_5$(BFEDA) in n-hexane

Complex	**CO-stretching frequencies (cm^{-1}) in hexane**				
	A_1^1	A_1^2	B_1	B_2	A_1^3
W(CO)$_5$(BFEDA)	2067.1	1966.8	1960.5	1922.1	1915.2

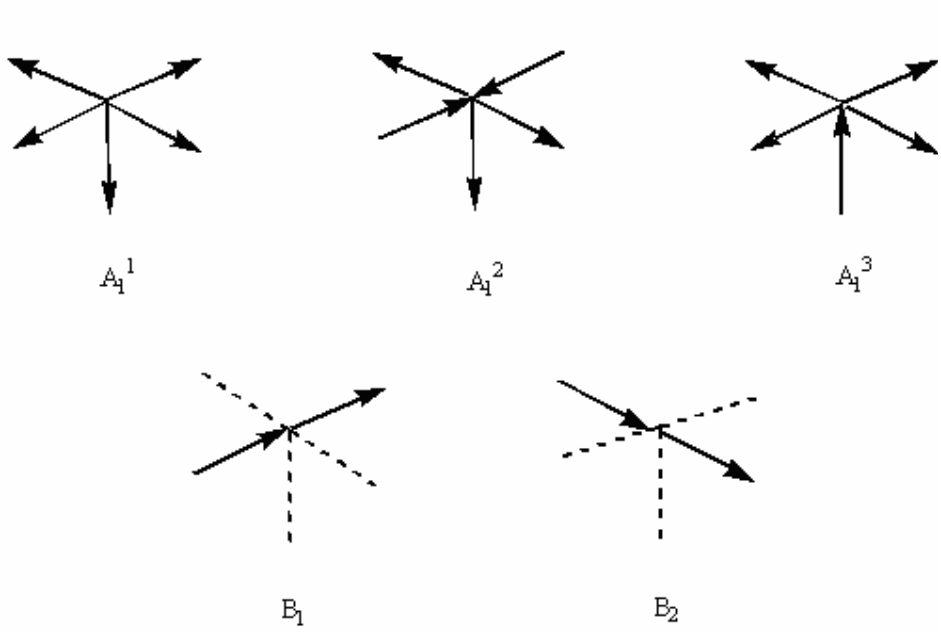

Figure 4.22. CO stretching vibrations of $W(CO)_5$(BFEDA)

In the imine region, the band at 1652 cm^{-1} is attributed to the C=N stretching of the uncoordinated side of the BFEDA ligand. On the other hand, the signal at 1605 cm^{-1} belongs to the C=N stretching, where N is bonded to the tungsten metal center.

The evidence of substitution of thf by BFEDA is the shifts of the CO stretching peaks to the lower frequencies; perhaps the clearest one is the shift of the signal at 2079 cm^{-1} to the 2067 cm^{-1}. This information also shows that, BFEDA molecule is a better σ-donor than thf. It donates electrons to the metal center, which causes a better interaction between metal and carbon due to the the σ dative and π-back bondings. Thus, the strength of the CO triple bond decreases and gives signals at lower frequencies.

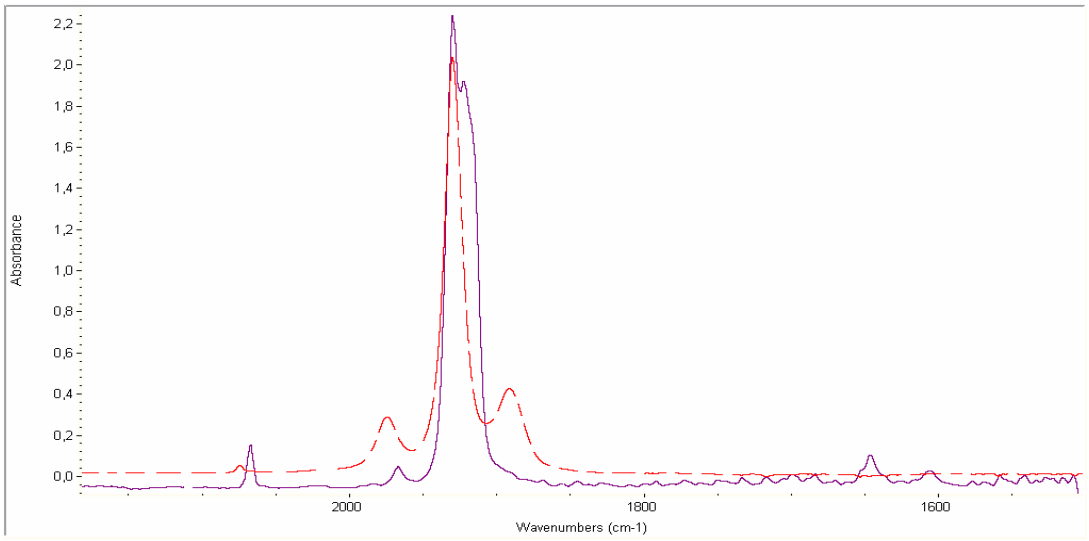

Figure 4.23. Comparison of $W(CO)_5$(thf) with $W(CO)_5$(BFEDA) by means of IR spectra. Dashed line denotes the spectrum of $W(CO)_5$(thf)

In the ^{1}H-NMR spectrum of the $W(CO)_5$(BFEDA) complex, the peak at 8.51 ppm and 8.16 ppm can be assigned to the protons of the imine groups, the proton of coordinated imine to the tungsten, and unbonded imine proton, respectively. Due to the electron withdrawing ability of the $W(CO)_5$ moiety, bonded imine proton is more deshielded, so is at lower field. Two unsubstituted ring protons are now seperated from each other, and observed at 4.00 and 3.91 ppm. Similarly, the α protons of both substituted rings give different peaks, at 4.55 and at 4.10 ppm. Furthermore, the β protons of two substituted rings resonate at 4.40 and 4.08 ppm. Lastly, the metylene protons resonate as triplets at 4.02 and 3.85 ppm. Note that, the signals at lower magnetic fields belong to the protons which are closer to the metal-imine bond.

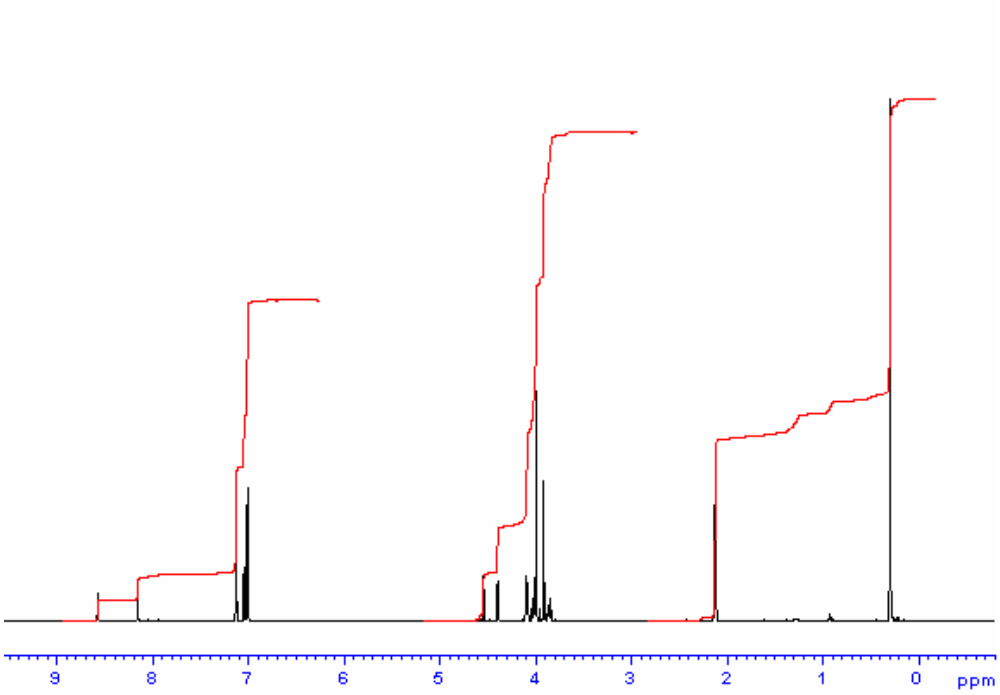

Figure 4.24. ^{1}H-NMR of the $W(CO)_5$(BFEDA) in d-toluene

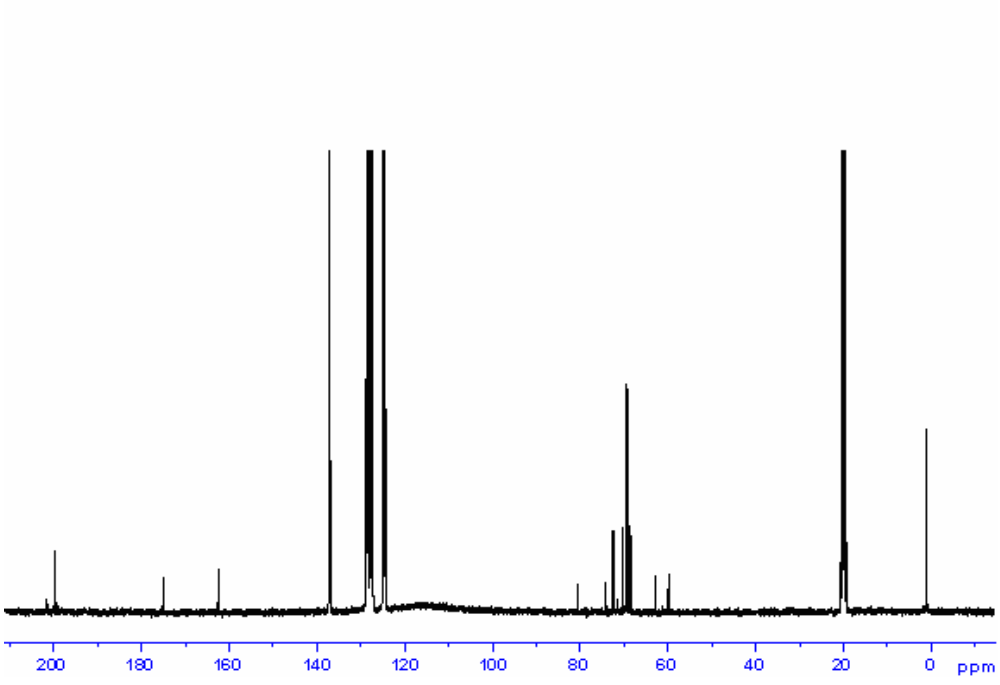

Figure 4.25. ^{13}C-{^{1}H}-NMR Spectrum of $W(CO)_5$(BFEDA) in d-toluene

The ^{13}C-{^{1}H}-NMR spectrum also proves the existence of the $W(CO)_5$(BFEDA) of the complex. The trans and the cis carbonyl groups give signals at 201.5 and 199.6 ppm respectively with a ratio of 1:4. Carbons of the imine groups have signals at 175.0 and 162.6 ppm, the imine which is bonded to the metal center is at lower field. When we make a comparison between pentacarbonyl(BFEDA)tungsten(0), tetracarbonyl(BFEDA)tungsten(0) and free BFEDA for the ipso carbons, we can conclude the the peak at 74.1 ppm belongs to the ipso carbon closer to the metal imine bond. The other one gives a peak at 80.6 ppm. In addition to these, α carbons of both substituted rings resonate at 70.3 and 72.7 ppm, whereas β carbons are at 68.6 and 72.4 ppm. Finally, methylene carbons give signals at 62.9 and 59.9 ppm, respectively.

When $W(CO)_5$(BFEDA) is dissolved in highly polar solvent, CH_2Cl_2, another CO group is replaced by the uncoordinated imine group of the BFEDA with a ring closure mechanism and forms $W(CO)_4$(BFEDA) complex. The reason for this event is the easily polarization of the M-CO bond and coordination of the solvent instead of another CO group at the first step. Since the metal-solvent bond is very weak, imine group can easily substitute the solvent. The formation of $W(CO)_4$(BFEDA) in CH_2Cl_2 can be seen more clearly in Figure 4.26. and from the IR spectra in Figure 4.27.

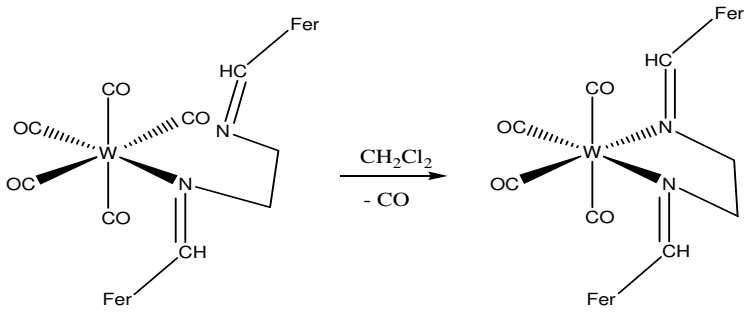

Figure 4.26. Ring closure reaction of $W(CO)_5$(BFEDA) to$W(CO)_4$(BFEDA) in CH_2Cl_2

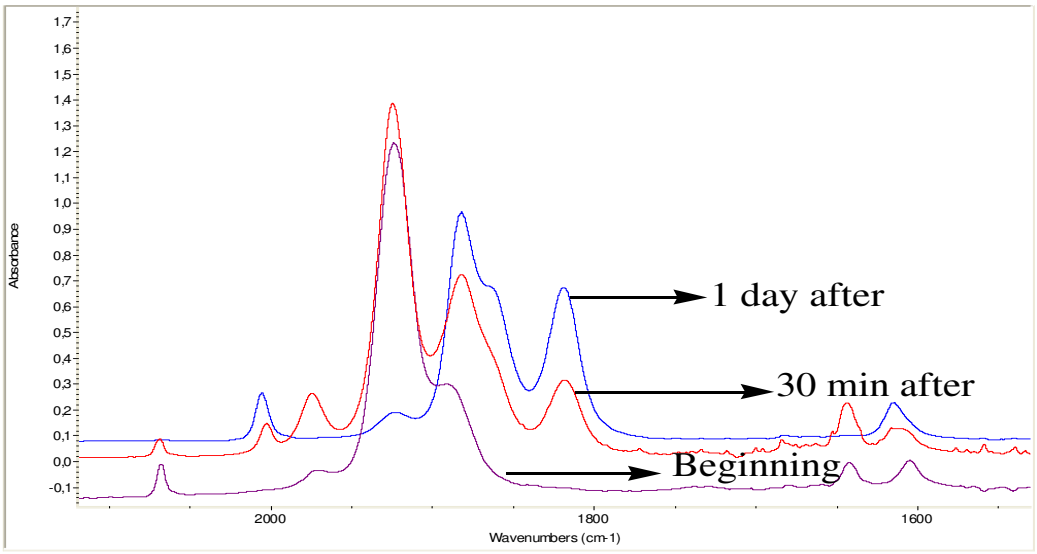

Figure 4.27. Formation of $W(CO)_4$(BFEDA) in CH_2Cl_2 from $W(CO)_5$(BFEDA) by ring closure

Similarly, the ligand exchange reaction of $W(CO)_5(\eta^2$-btmse) with BFEDA in CH_2Cl_2 gives mainly $W(CO)_4$(BFEDA) complex as it was mentioned above. As a consequence of these facts, when we attempted to prepare $W(CO)_5$(BFEDA) by substitution of $W(CO)_5(\eta^2$-btmse) with BFEDA, we used a less polar solvent, toluene, instead of CH_2Cl_2.

4.4. Comparison of $M(CO)_4$(BFEDA) complexes (M: Cr, Mo, W)

The chromium and the molybdenum analogoues of group 6 metal $M(CO)_4$(BFEDA) complexes have already been studied in our research group.[29,30]

The infrared spectra of three $M(CO)_4$(BFEDA) complexes (M: Cr, Mo, W) exhibits four IR active bands in CO stretching region with vibrational modes of $2A_1+B_1+B_2$. Thus, the local symmetry of the $M(CO)_4$ moiety is C_{2v}. The CO stretching frequencies for the three $M(CO)_4$(BFEDA) complexes are listed in Table 4.5.

Table 4.5. The CO and C=N stretching frequencies (cm^{-1}) of $M(CO)_4$(BFEDA) complexes (M: Cr, Mo, W) in CH_2Cl_2.

	ν(CO)				**ν(C=N)**
Complex	$A_1^{(2)}$	B_1	$A_1^{(1)}$	B_2	
$Cr(CO)_4$(BFEDA)	2004	1887	1870	1822	1620
$Mo(CO)_4$(BFEDA)	2011	1894	1875	1824	1618
$W(CO)_4$(BFEDA)	2005	1882	1863	1819	1614

As it is seen from the Table 4.5., the C=N stretching frequencies decrease from Cr to W complexes. This shows that the π-back bonding increases in the same order.

^{1}H-NMR chemical shifts of group 6 metal $M(CO)_4$(BFEDA) complexes are given in Table 4.6. Note that the chemical shifts are very close to each other.

Table 4.6. ^{1}H-NMR chemical shifts of $M(CO)_4$(BFEDA) (M: Cr, Mo, W) complexes

$M(CO)_4$(BFEDA)	$\mathbf{H}_\alpha$	$\mathbf{H}_\beta$	$\mathbf{H}_{unsubs.}$	**H**C=N	-C**H**$_2$-
Cr	5.09	4.58	4.25	8.50	3.66
Mo	5.15	4.61	4.27	8.44	3.76
W	5.16	4.64	4.27	8.43	3.84

Table 4.7. shows the ^{13}C-NMR chemical shifts and the coordination shifts of $M(CO)_4$(BFEDA) complexes. The decrease in the coordination shifts of ipso carbons states that the degree of π-back bonding from metal to BFEDA increases going from chromium to tungsten metal. In addition, deshielding of the imine

carbons upon coordination of free BFEDA molecule to the metal centers decrease, going from chromium to molybdenum and tungsten. This observation is also an indication of the increasing π- interaction between central metal atom and BFEDA ligand by going down in group 6 metals.

Table 4.7. Chemical shifts (δ, ppm) of $M(CO)_4$(BFEDA) complexes. The coordination shifts are given in parentheses with respect to the free BFEDA molecule (Δδ, ppm).

$M(CO)_4$(BFEDA)	$\mathbf{C}_{ipso}$	$\mathbf{C}_{\alpha}$	$\mathbf{C}_{\beta}$	$\mathbf{C}_{uns.}$	H**C**=N	**-C**H_2-
Cr	78.2 (-2.7)	72.5 (1.8)	72.3 (3.5)	70.0 (0.3)	171.1 (8.4)	66.1 (3.5)
Mo	77.7 (-3.2)	72.6 (1.9)	72.3 (3.5)	70.1 (0.4)	170.8 (8.1)	66.6 (4.0)
W	77.2 (-3.7)	72.6 (1.9)	72.4 (3.6)	69.8 (0.1)	170.6 (7.9)	67.5 (4.9)

The UV-VIS spectra of $Cr(CO)_4$(BFEDA) and $Mo(CO)_4$(BFEDA) complexes show two charge transfer transitions, whereas the tungsten analogue exhibits one more peak at 250 nm. On the other hand, the d-d transition of chromium metal can not be observed in $Cr(CO)_4$(BFEDA).

Table 4.8. The electronic absorption bands of $M(CO)_4$ (BFEDA) (M: Cr, Mo, W) complexes in CH_2Cl_2 at room temperature

$M(CO)_4$(BFEDA)	CT	CT	d-d transition of central metal	d-d transition of iron center
Cr	233	269	-	340
Mo	236	259	304	348, 480
W	237	250, 277	306	351, 472

Electrochemical behaviors of $M(CO)_4$(BFEDA) complexes were investigated by cyclic voltammogram in the same solvent-electroyte couple at a voltage scan rate of 100 mV/s (Figure 4.28.).

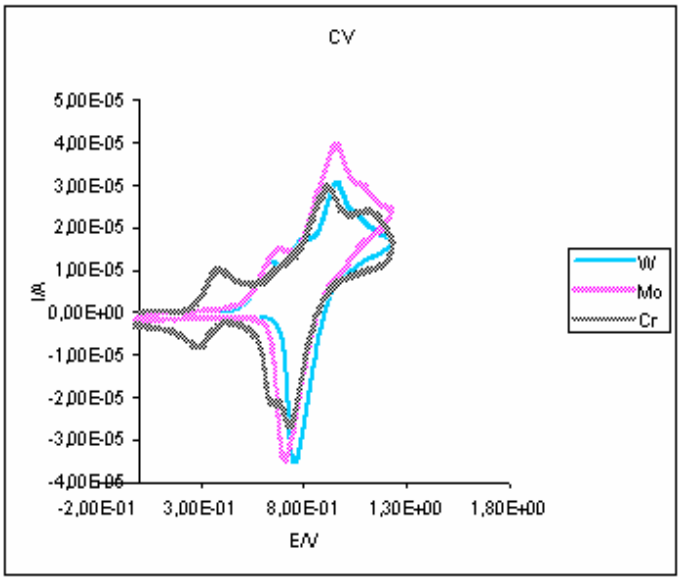

Figure 4.28. Cyclic voltammogram of $M(CO)_4$(BFEDA) (M: Cr, Mo, W) complexes taken in CH_2Cl_2 at room temperature with SCE as reference

The first oxidation peaks in CV show that $Cr(CO)_4$(BFEDA) complex has a reversible oxidation of Cr(0) to Cr(I), whereas the oxidation of molybdenum and the tungsten analogues from M(0) to M(I) are irreversible. These irreversible oxidations of molybdenum and tungsten metals have been reported in the literature[47] and deduced to the poor stability of oxidation products of them. The first oxidation potentials of central metals in $M(CO)_4$(BFEDA) complexes, increase from Cr to Mo and W. However, the increases in oxidation potentials are much greater for Cr- Mo than the Mo-W case. This observation is resulted from lanthanide contraction.

The separation of the potentials of two ferrocene moieties oxidations increases from Cr to Mo and W analogue. That is, the electronic communication between two ferrocene increases. In addition to IR and ^{13}C-NMR observations, this also proves a better π-interaction occurs in $W(CO)_4$(BFEDA) than the chromium and the molybdenum analogues of BFEDA molecule.

To enlighten the mechanism of the oxidations in these complexes, the constant potential electrolysis followed by in-situ UV-VIS spectroscopy was performed. For the electrolysis of the $Cr(CO)_4$(BFEDA) complex, only three electron transfers were observed. First, the oxidation of Cr metal center, from Cr(0) to Cr(I) occurred. The second and the third oxidations were attributed to the oxidations of iron metal centers from Fe(II) to Fe(III). Due to instability of $Cr(CO)_4$(BFEDA) complex, oxidation of more than three electron could not be achieved. The schematic representation of oxidation mechanism of the $Cr(CO)_4$(BFEDA) complex is shown below :

1. Oxidation of chromium fragment, changing the oxidation state of chromium from (0) to (+1):

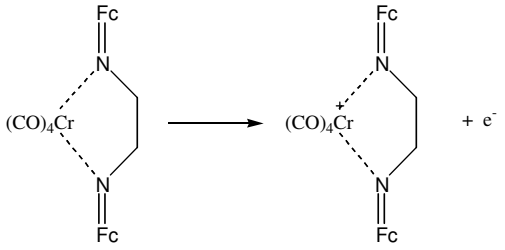

2. Oxidation of first ferrocene moiety, changing the oxidation state of iron center from (+2) to (+3):

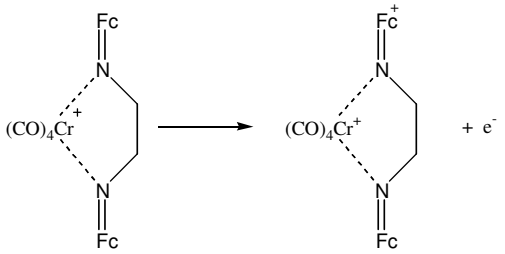

3. Oxidation of second ferrocene moiety, changing the oxidation state of iron center from (+2) to (+3):

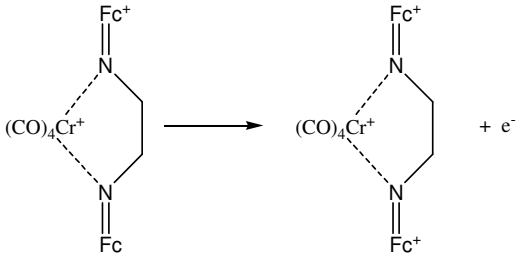

On the other hand, five-electron transfer was expected for both molybdenum and tungsten analogues. Although, the oxidation was carried until the end of the fifth electron passage for the Mo complex, the electrolysis was

stopped after the fourth electron transfer in $W(CO)_4$(BFEDA) complex because the complex started to decompose. The oxidation steps in both molybdenum and tungsten complexes show similarities. In both case, the first two-electron passage happens at the iron centers of the ferrocene moiety. Then, the central metals start to be oxidized. The oxidation mechanism of both $Mo(CO)_4$(BFEDA), $W(CO)_4$(BFEDA) complexes are shown in section 4.2.

CHAPTER 5

CONCLUSIONS

The N,N'-bis(ferrocenylmethylene)ethylenediamine (BFEDA) was prepared from the condensation reaction of ferrocenecarboxyaldehyde and ethylenediamine by using a dean-stark apparatus in benzene solution and characterized by IR, Raman and NMR spectroscopies. This diimine molecule containing two ferrocenyl moieties was employed in the synthesis of tetracarbonyl [bis(ferrocenylmethylene)ethylenediamine)]tungsten(0), $W(CO)_4$(BFEDA) and pentacarbonyl[bis(ferrocenylmethylene)ethylenediamine)]tungsten(0), $W(CO)_5$(BFEDA) complexes. The bidentate property of the BFEDA was used for the preparation of the $W(CO)_4$(BFEDA).

Both IR and ^{13}C-$\{^1H\}$-NMR spectra show that, BFEDA molecule is a σ-donor ligand rather than a π-acceptor ligand. This σ-donation ability of BFEDA upon coordination causes a decrease in the electron density of all the atoms in the BFEDA fragment except ipso carbons. Another consequence of the σ-donation from BFEDA to $W(CO)_4$ or $W(CO)_5$ fragment is the weakening of the triple bond of the carbonyl groups.

The $W(CO)_4$(BFEDA) complex was synthesized by two different substitution reactions as described in experimental part. However, the best yield was obtained by the thermal substitution reaction of $W(CO)_5(\eta^2$-btmse) complex with BFEDA in CH_2Cl_2. The complex was fully characterized by elemental analysis, UV-VIS, IR, ^1H-NMR, ^{13}C-$\{^1H\}$-NMR and Mass spectroscopies. The IR spectrum of $W(CO)_4$(BFEDA) shows four CO stretching bands which is an evidence of C_{2v} local symmetry for $W(CO)_4$ moiety and one C=N stretching band. The C_{2v} symmetry of $W(CO)_4$ fragment was also proved by ^1H-NMR and ^{13}C-$\{^1H\}$-NMR spectroscopies.

The electrochemical properties of $W(CO)_4$(BFEDA) was studied by using cyclic voltammetry and differential pulse voltammetry. The mechanism of electrode reaction was investigated by in-situ UV-VIS spectroscopy during electrolysis. Cyclic voltammogram reveals that first tungsten metal is oxidized. Next, the ferrocene centers undergo one electron oxidations from Fe^{2+} to Fe^{3+}. Lastly, tungsten is oxidized again from W^{+} to W^{3+}. Shortly, five electron passages happen. However, in the electrolysis, an intramolecular electron transfer occurs from one iron center to tungsten metal and reduces it back to zero state. As a conclusion, the $W(CO)_4$(BFEDA) complex has three redox centers which are two iron and one tungsten center and they communicate with each other via π conjugation.

The $W(CO)_5$(BFEDA) complex was synthesized either by substitution reaction of thf with BFEDA in photogenerated $W(CO)_5$(thf) solution or by the thermal substitution reaction of $W(CO)_5(\eta^2$-btmse) complex with BFEDA in toluene. However the best yield was obtained from the substitution of thf with BFEDA. The complex was fully characterized by IR, ^{1}H-NMR, ^{13}C-{^{1}H}-NMR spectroscopies. Five observable bands can prove that $W(CO)_5$(BFEDA) complex has a local symmetry of C_{2v} for the $W(CO)_5$ moiety. The spectrum also displays two C=N bands one for the imine attached to the tungsten and the other for the uncoordinated imine group. ^{1}H-NMR, ^{13}C-{^{1}H}-NMR spectra are also in a good accord with the infrared spectrum and show the existence of the complex.

It is found that in a highly polar solvent like CH_2Cl_2, the $W(CO)_5$(BFEDA) complex is not stable and changes its coordination to $W(CO)_4$(BFEDA) by the replacement of another CO group with the unbonded imine group of the BFEDA by a ring closure mechanism. Due to this instability, electrochemical behaviour of the molecule can not be investigated.

REFERENCES

1 Swaddle, T.W., *"Applied Inorganic Chemistry "* , University of Calgary Press, Calgary, 1992

2 Miessler G.L.; Tarr, D.A., *" Inorganic Chemistry"* , 2nd edition, Prentice Hall Press, New Jersey, 1998

3 Swaddle, T.W., *"Inorganic Chemistry"*, Acedemic Press, California, USA, 1997

4 Pruchnik, F.P., *"Organometallic Chemistry of the Transition Elements*", Plenum Press, New York, 1990

5 Süss-Fink,G.; Meister, G., *Adv. Organomet. Chem*. ,35, (1993), 41.

6 Rochow, E.G.; Hurd, D.T.; Lewis, R.N., *" the Chemistry of Organometallic Compounds"*, John Wiley & Sons, New York, 1957

7 Wender, I.; Pino, P., "*Organic Synthesis via Metal Carbonyls"*, volume 1, Interscience Publishers, USA, 1968

8 Huheey, J.E.; Keiter, E.A.; Keiter, R.L., "*Inorganic Chemistry- Principles of Structure and Reactivity"*, 4th edition, Harpercollins College Publishers, New York, 1993

9 Braterman P.S., *"Metal Carbonyl Spectra"*, Academic Press ,London, 1975

10 Crabtree, R.H., *" The Organometallic Chemistry of the Transition Metals"*, John Wiley & Sons Inc., New York, 1998

11 Elschenbroich, C.; Salzer A., *"Organometallics"*, 2nd edition., VCH, Weinheim, 1992

12 Jordan R.B., "*Reaction Mechanisms of Inorganic and Organometallic Systems*", Oxford University Press, Oxford, 1991

13 Coates, G.E., *"Organo-Metallic Compounds"*, John Wiley & Sons, 1956

14 Togni, A.; Hayashi, T., *"Ferrocenes: Homogeneous Catalysis, Organic Synthesis, Materials Science",* VCH, Weinheim, 1995

15 Gmelin Handbook of Inorganic and Organometallic Chemistry, *Fe Organic Compounds,* 8th ed., vol. A10, Springer, Berlin, 1991

16 Bear, P.D.; Smith, D.K., *Prog. Inorg. Chem*., 46 (1997) 1

17 Miller, J.S.; Epstein, A.J., *Angew. Chem. Int. Ed. Engl*, 34 (1994) 385

18 Long, N.J., *Angew. Chem. Int. Ed. Engl*., 35 (1995) 21

19 Coles, H.J.; Meyer, S.; Lehmann, P. ; Deschenaux, R.; Juaslin, I., *J. Mater. Chem.*, 9 (1999) 1085

20 Astruc, D., *New. J. Chem.,* 16 (1992) 305

21 Astruc, D., *Acc. Chem. Res*., 30 (1997) 383

22 Beer, P.D*., Acc. Chem. Res*., 31 (1998) 71

23 Bildstein, B.; Malaun, M.; Kopacka, H.; Fontani, M.; Zanello, P., *Inorg. Chimica Acta*, 300-302 (2000) 16

24 Stufkens, D.J., *Coord. Chem. Rev*., 104 (1990) 39-112

25 Brunner, H.; Herrman, W.A., *Chem. Ber*., 105 (1972) 770-783

26 Özkar, S.; Grevels, F.-W.; Kayran, C., *Organometallics*, 13 (1994) 2937

27 Benito, A.; Cano, J.; Manez, R. M.; Soto, J.; Paya, J.; Lloret, F.; Julve, M.;

Faus, J.; Marcos, M. D.; *Inorg. Chem.*, 32 (1993) 1197.

28 Zhang et. al. *Synth. React. Inorg. Met.-Org. Chem*., 31(6) (2001) 1054

29 Akyol, C., *Master Dissertation*, METU, 2005

30 Koçak, S., *Master Dissertation*, METU, 2005

31 Plambeck, J.A., "*Electroanalytical Chemistry, Basic Principles and Applications"*, John Wiley & Sons, New York, 1982

32 Connely, N.G.; Geiger W.E., " *Advances in Organometallic Chemistry*", Acedemic Press, New York, 1984

33 Gosser, D. K.; "*Cyclic Voltammetry"*, VCH Verlagsgesellschaft, USA, 1993.

34 Shriver, D.F.; Atkins, P.W.; Langford, C.H., *" Inorganic Chemistry"*, 2nd ed., Oxford University Press, 1994

35 Mackay, K.M.; Mackay, R.A., *"Modern Inorganic Chemistry"*, 3rd ed., Int. Textbook Co., London, 1981

36 Purcell, K.F.; Kotz, J.C., *"Inorganic Chemistry"*, W.B. Saunders Co., Philadelphia, 1977

37 Okan, E., Master Dissertation, METU, 1998

38 Solomons, G.; Fryhle, C., "*Organic Chemistry", 7th Edition*, John Wiley& Sons, Inc., 2000.

39 Bochmann M.; "*Organometallics 2-Complexes with Transition Metal-Carbon π-Bonds"* , Oxford University Press , Oxford , 1994

40 Dewar M.J.S. ; *Bull.Soc.Chim.France* , 18 (1951) C71-79

41 Chatt J., Duncanson L.A.; *J.Chem.Soc. (London)* , 73 (1953) 2939

42 Bosque, R.; Lopez, C.; Sales, J.; Solans, X.; Font-Bardia, M., *J. Chem. Soc.*, Dalton Trans., 1994, 735.

43 Marie-Madeleine Rohmer et al.; Chem. Phys. Let., 29 (1974) 466

44 Gosser, D.K., *"Cyclic Voltammetry",* VCH Verlagsgesellshaft, USA, 1993

45 Saldamlı, S.; Doctoral Dissertation, METU ; 2001

46 Grevels, F. W.; Kerpen, K.; Klotzbücher, W. E.; Schaffner, K.; Goddard, R.; Weimann, B.; Özkar, S.; Kayran, C., *Organometallics,* , 20 (2001) 4775.

47 Wong, W.Y.; Cheung, S.H.; Loe, S.M.; Leung, S.Y., J. Organomet. Chem., 596 (2000) 36

APPENDIX

UV-VIS spectra of 5.0 x 10^{-5} M free BFEDA molecule taken in CH_2Cl_2 solution at room temperature

Wavelength	**Molar Absorptivity (L / mol.cm)**
230	2.965 x 10^4
274	1.650 x 10^4
330	0.275 x 10^4
460	0.105 x 10^4

UV-VIS spectra of 5.0 x 10^{-5} M $W(CO)_4$(BFEDA) molecule taken in CH_2Cl_2 solution at room temperature

Wavelength	**Molar Absorptivity (L / mol.cm)**
237	3.528 x 10^4
250	3.372 x 10^4
277	1.832 x 10^4
306	0.964 x 10^4
351	0.110 x 10^4
472	0.280 x 10^4